Seismic microzonation for Muscat region, Sultanate of Oman

Nat Hazards (2013) 69:1919–1950
DOI 10.1007/s11069-013-0785-9

ORIGINAL PAPER

Seismic microzonation for Muscat region, Sultanate of Oman

I. El-Hussain · A. Deif · K. Al-Jabri · A. M. E. Mohamed · G. Al-Rawas · M. N. Toksöz · N. Sundararajan · S. El-Hady · S. Al-Hashmi · K. Al-Toubi · M. Al-Saifi · Z. Al-Habsi

Received: 22 September 2012 / Accepted: 5 July 2013 / Published online: 19 July 2013

Abstract Site characterization was carried out for Muscat region using the ambient noise measurements applying the horizontal-to-vertical spectral ratio (HVSR) technique and using active seismic survey utilizing the multichannel analysis of surface waves (MASW) of survey data. Microtremors measurements were carried out at 459 sites using short-period sensors. This extensive survey allowed the fundamental resonance frequency of the soft soil to be mapped and areas prone to site amplification to be identified. The results indicate a progressive decrease in the fundamental resonance frequencies from the southern and eastern parts, where the bedrock outcrops, toward the northern coast where a thickness of sedimentary cover is present. Shear wave velocity (Vs) was evaluated using the 2-D MASW at carefully selected 99 representative sites in Muscat. These 99 sites were investigated with survey lines of 52 m length. 1-D and interpolated 2-D profiles were generated up to a depth range 20–40 m. The vertical Vs soundings were used in the SHAKE91 software in combination with suitable seismic input strong motion records to obtain the soil effect. Most of the study area has amplification values less than 2.0 for all

I. El-Hussain (✉) · A. Deif · S. Al-Hashmi · K. Al-Toubi · M. Al-Saifi · Z. Al-Habsi
Earthquake Monitoring Center, Sultan Qaboos University, Muscat, Oman
e-mail: elhussain@squ.edu.om

A. Deif · A. M. E. Mohamed · S. El-Hady
National Research Institute of Astronomy and Geophysics (NRIAG), Helwan, Cairo, Egypt

K. Al-Jabri · G. Al-Rawas
Department of Civil and Architectural Engineering, Sultan Qaboos University, Muscat, Oman

M. N. Toksöz
Massachusetts Institute of Technology, Cambridge, MA, USA

N. Sundararajan
Earth Science Department, Sultan Qaboos University, Muscat, Oman

S. El-Hady
Faculty of Earth Science, Geophysics Department, King Abdulaziz University, Jeddah, Saudi Arabia

the considered spectral periods. The estimated fundamental frequencies obtained using the H/V spectral ratio method and using SHAKE91 are found to be in a relatively good agreement. Maps of spectral amplification, earthquake characteristics on the ground surface for peak ground and spectral accelerations at 0.1, 0.2, 0.3, 1.0, and 2.0 s, for 475 years return period are produced. The surface ground motion maps show that the hazard level is moderate with expected PGA in the range 0.059–0.145 g for 475 years return period.

Keywords Muscat · Spectral ratio · Site amplification · Shear wave velocity · Seismic microzonation

1 Introduction

Oman occupies the southeastern corner of the Arabian plate and is surrounded by relatively high active tectonic zones (Fig. 1). Active tectonics of the region is dominated by the collision of the Arabian plate with the Eurasian plate along the Zagros and Bitlis thrust systems, subduction of the Arabian plate beneath the Eurasian plate along Makran subduction zone, the transformation of Owen fracture zone that separates the Arabian and the Indian plates, rifting and seafloor spreading in the Gulf of Aden.

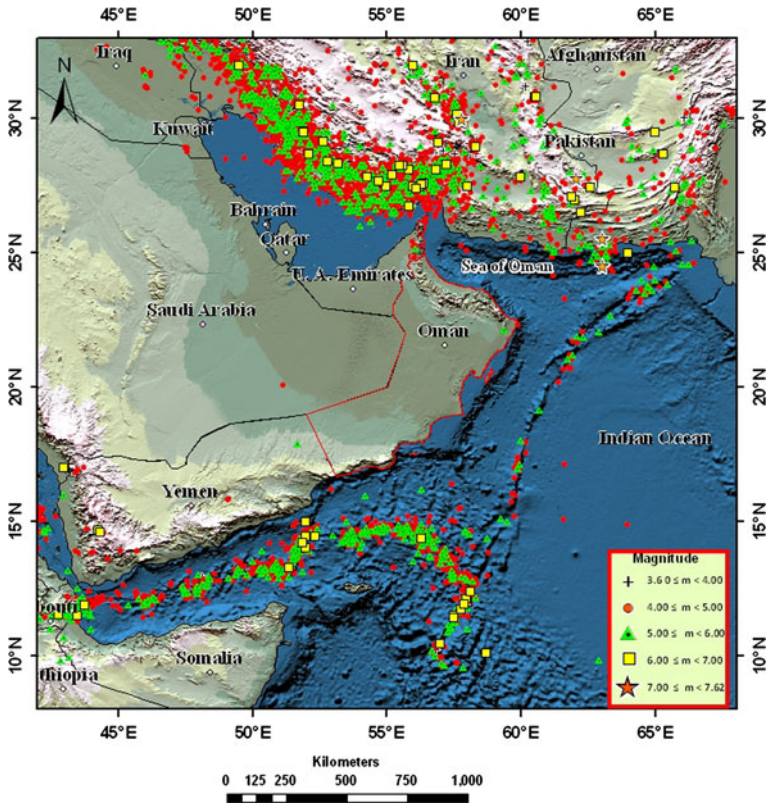

Fig. 1 Instrumental seismicity of Sultanate of Oman and its surrounding

The constructive interference of the trapped seismic waves between the soft sediments and the hard rock can result in significant amplification of the earthquake ground motion. The spatial distribution variability of the earthquake ground motion amplification yields a dramatic change in the severity of damage to the man-made structures. The site amplification phenomenon documented during the earthquake of Mexico, 1985, highlighted the possibility of severe ground motions on soft soil sites located at large distance from causative faults. Lower-frequency components of the generated seismic waves can travel very far with long duration and without much attenuation causing resonant vibrations in structures with low natural frequencies. Therefore, large remote earthquakes from Zagros and Makran seismic zones can have damaging effect on the tall buildings rested on soft soils in the Arabian Gulf region.

Muscat is the capital city of the Sultanate of Oman located in the northeastern part of the Sultanate between the Oman Mountains and the coast of the Sea of Oman. It houses important government and industrial facilities. Some of these installations are located directly on bedrocks, while others are located on soft soils and sediments. Muscat Governorate population is 28 % of the total Omani population, and its number of households is approximately 30 % of the total Omani households.

The main factor controlling the earthquake hazard for Muscat region is undoubtedly the proximity of the Makran seismic zone and the Oman Mountains (El-Hussain et al. 2012a). Historically, Muscat was affected by a medium earthquake of estimated magnitude $M_S = 5.5$ in 1883, which led to the damage of nine villages (Ambraseys et al. 1994). This scenario could be worsened due to the larger extent of the city and the probable site amplifications associated with the soft sediments at the northern part of the region overlying competent bedrock. Due to this extension, many new residential, industrial, and touristic communities were constructed, and the importance of characterizing the site effects is well realized.

The fundamental frequency, which depends on the soil thickness and shear wave velocity of the soil, provides a very useful indication of the frequency of vibration at which the most significant amplification can be expected. In the current study, the Nakamura technique (Nakamura 1989) is used to estimate the fundamental resonance frequency of soft soils at Muscat. This technique characterizes each site by the ratio (H/V) of the Fourier spectra of the horizontal and vertical components of ambient noise measurements made with a single, 3-component seismograph. Lachet and Bard (1995) concluded that Nakamura's technique may be used to determine the fundamental resonance frequency of a soft layer, but it fails to accurately predict the amplification coefficient. Therefore, performing a large number of noise measurements over a region of interest allows a map of the resonance frequencies to be obtained.

Shear wave velocity (Vs) is a key factor in the site response analyses (Borcherdt 1970). In the current study, 99 2-D multichannel analysis of surface waves (MASW; Miller et al. 1999; Xia et al. 2000) surveys were carried out in representative sites of the study area to estimate the shear wave velocity profiles. The MASW technique is based on the inversion of the Rayleigh wave dispersion curves, which are proved to obtain the characterization of the local shear wave velocity profile with a good accuracy (Tokimatsu et al. 1992; Ohori et al. 2002; Parolai et al. 2004). The inversion process requires the definition of an initial depth model, which is estimated through a conventional P-wave shallow seismic refraction measurement at each site of interest. The P-wave velocity obtained from the shallow seismic refraction technique is transformed into shear wave velocity. The transformed shear wave velocities and their corresponding depths are the initial depth models for the MASW analyses.

The resulted Vs profiles were then used in the SHAKE91 software in EZ-FRISK 7.62 package in combination with seismic input motion to obtain site response and amplification spectra at each of the studied 99 sites. Real strong motion records were obtained through searching in the strong motion databases to find the strong motion records that obey the searching criteria: magnitude, distance, duration, and mechanism. This initial strong motion record was modified using the spectral matching approach (Al Atik and Abrahamson 2010) to make the time series consistent with the design response spectrum in the Muscat area. This modified time series is used as an input for the SHAKE91 software.

Maps of spectral amplification are presented for earthquake characteristics on the ground surface for peak ground and spectral accelerations at 0.1, 0.2, 0.3, 1.0 and 2.0 s, for 475 years return period, based on the regional earthquake hazard model developed by El-Hussain et al. (2012a).

2 Geologic setting of Muscat region

The surface geology of Muscat regions reveals great variety of rocks and sediments. The bedrocks, which concentrate in the eastern and southern parts of the regions, consist of carbonates, ophiolite, tectonic mélange, tertiary sandstones, and limestones. These bedrocks provide variety of materials that make up the Quaternary and recent deposits. The Quaternary deposits are generally a firm-looking cream-colored deposit that often shows the marks of quarrying. These are deposits of Aeolian sand dunes. Figure 2 shows surface geology of Muscat region.

The recent (Holocene) deposits are dominating the low-lying areas along the coast and in wadis, where a system of unconsolidated modern deposit exists. Sandy beaches extend from Al-Qurum westward to As-Seeb with variable inland depth. Areas in Al-Qurum and north of Muscat international airport consist of depression with recent clay and silt sedimentation with shallow ground water depth that turn these areas into Sabkhas (Fig. 2). Features of bar

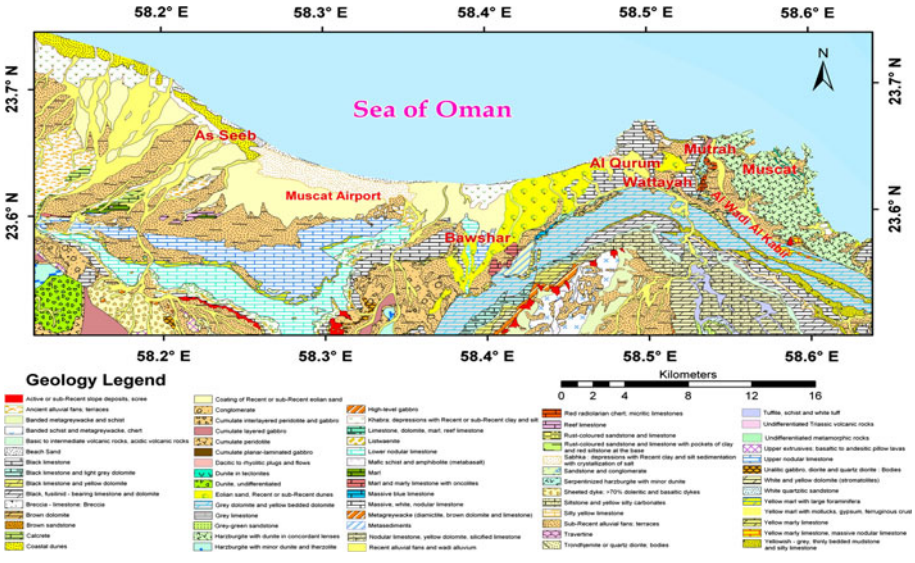

Fig. 2 Surface geology of Muscat region

sands, sand dunes, a tidal channel system, delta channels, and (in the tidal channel) a well-developed point bar do exist in Muscat and its surrounding. In general, the surface sediment materials in Muscat are dense to very stiff mixture of clay, silt, sand, gravel, and rock fragment material except the top soil layer in some places (BRGM/MPM 1986).

3 Fundamental resonance frequency based on microtremors measurements

The technique that first applied by Nogoshi and Igarashi (1970, 1971) and popularized by Nakamura (1989), using horizontal to vertical spectral ratios (H/V) of the microtremors, was used to estimate the fundamental resonant frequency across the entire area of interest. Nakamura (1989) explained, based upon qualitative arguments, that the amplitude of the horizontal to vertical (H/V) spectral ratio gives a reliable estimation of the site response to vertically incident shear waves. The efficacy and theoretical assumptions to the H/V Nakamura technique are debatable because some authors such as Lermo and Chavez-Garcia (1994), Lachet and Bard (1994) show that H/V ratios are related to the ellipticity of Rayleigh waves. Nakamura (1996), in a later paper, reconsidered his explanation regarding the origin of microtremors and allowed a greater role for surface waves.

Several experimental studies (e.g., Lermo and Chavez-Garcia 1994; Theodulidis and Bard 1995; Malagnini et al. 1996; Konno and Ohmachi 1998; Zaslavsky et al. 2003; Parolai et al. 2004; Mohamed et al. 2008; Surve and Mohan 2010) found that the H/V technique provides reliable estimation of the fundamental frequency of soft deposits. In order to conduct seismic microzonation of Muscat city in terms of resonance frequency of the soil column, 459 field experiments using single-station microtremor measurements (Nakamura technique) were carried out (Fig. 3).

3.1 Field measurements

Four digital seismographs equipped with 24-bit data acquisition systems (ORION, and Quanterra Q330), which are modern field portable and highly flexible digital seismographic

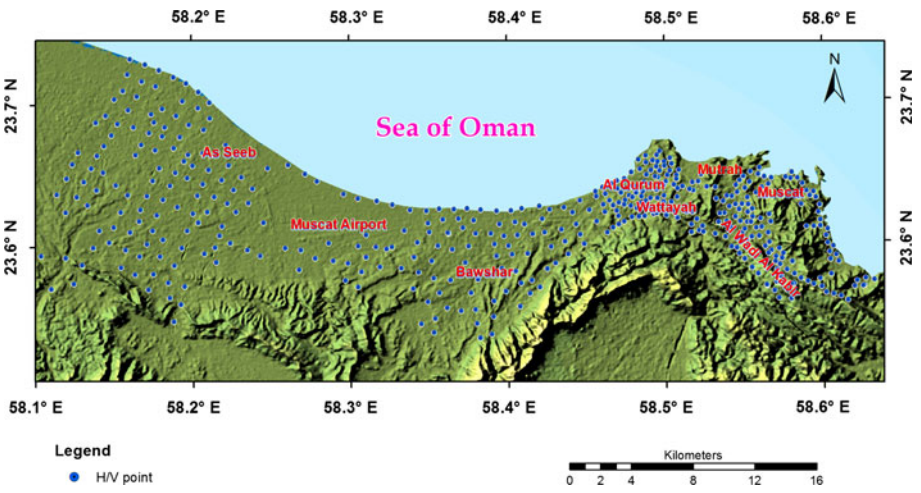

Fig. 3 Locations of microtremors surveys in Muscat region

recorders, and short-period 3-component seismometers (MARK L4-3D) with a natural frequency of 1 Hz were used for data acquisition. The sampling rate of recording in all cases was 100 Hz. Measurements for at least 40 min at each site were done.

3.2 Data processing

The raw data were processed using the GEOPSY software developed within the European project SESAME (2004). For each site, the microtremors record was corrected for the baseline effect to guarantee the stationary assumption validity. Various number of non-overlapping windows with 25-s (2,500 samples) duration were selected among the quietest parts of the recorded signals (for each site, at least 10 windows were used). This is done using the STA/LTA anti-trigger algorithm. This time window is sufficiently long to provide stable results in the studied range of frequency (0.4–25 Hz). The time series was tapered with a 10 % cosine taper, and an amplitude spectrum is computed using the fast Fourier transform (FFT) for all the three components.

These FFT spectra were smoothed with the "Konno-Ohmachi 1998" algorithm with a bandwidth coefficient value equal to 40. "Konno-Ohmachi 1998" smoothing with constant bandwidth in a logarithmic scale is recommended because this smoothing function preserves the different number of points at low and high frequency. Boore (2008) shows that Konno and Ohmachi smoothing function seems to work well; the smoothing operation is somewhat slower than using a boxcar and triangular weighting over the interval (because of the evaluations of sin and log), but that is probably not relevant for most applications.

Constant bandwidth smoothing may distort low frequency peaks (i.e., at frequencies lower than 1 Hz). Fortunately, all the fundamental resonance frequency in the area of interest is higher than 1.8 Hz, and thus, this constant bandwidth coefficient has no effect on the yielded spectra. The smoothing of the spectra, as shown by several authors (e.g., Bindi et al. 2000; Picozzi et al. 2005), allows the stabilization of the H/V curves, avoiding the presence of spurious peak due to seismic or instrumental or numerical noise.

Then, the two horizontal components were merged together using geometric mean option as in Eq. (1):

$$H = \left(\left|x_f.y_f\right|\right)^{0.5} \tag{1}$$

where H is the horizontal component computed by geometric mean, x_f is the modulus of spectra of the N–S component, and y_f is the modulus of spectra of the E–W component. The mean of the two horizontal components could be calculated also using cross-spectral ratios which show reliable estimates of site amplification (Safak 1997). The horizontal FFT spectra of the 25-s data subsets were divided by the vertical ones yielding number of H/V's curves for each site. These H/V's are then averaged and standard deviations at each frequency of interest are calculated. The resonance frequency and the corresponding amplitude at each site could then be determined.

The presence of strong sources acting during the recordings may be revealed also by means of a directional analysis of the H/V curves. In order to perform such analysis, the horizontal components of motions are rotated in the 0°–180° range and are combined for the H/V computation at regular intervals. This is very useful to check whether a site is 1-D. Similar to rotated H/V, the spectra with horizontal components spanning different azimuths are computed. Azimuth is regularly counted clockwise from the north. This is useful to check the direction of energy release. The rotated spectra and rotated H/V curves were conducted for all the sites of interest.

Finally, all the peaks that appeared on the H/V curves were tested for their origin (natural or industrial) and for their reliability. The peak is considered of industrial origin if: they exist over a significant area; raw Fourier spectra exhibit sharp peaks at the same frequency for all the three recorded components; peaks get sharper with decreasing smoothing; and the random decrement technique (Dunand et al. 2002) indicates very low damping ($z < 1$ %) around the frequency of interest. Peaks that proved to be of industrial origin were discarded from the interpretation because they are not related to the site characterization.

Stringent criteria for reliability of results were adopted (SESAME 2004). The primary requirement for reliable H/V curves is the stability of the H/V curves. Thus, it is ensured that at least 10 significant cycles were present in each window in the frequency of interest, at least 10 windows were taken, and low level of scattering in each window was considered. The reliable H/V curves next require to satisfy the stability criteria for a clear peak which is related to several characteristics, i.e., the amplitude of the H/V peak and its relative value with respect to the H/V value in other frequency bands, the relative value of the standard deviation and the standard deviation of the peak frequency from individual windows (SESAME 2004). H/V curves that are not satisfying the primary criteria for clear curves and the stability criteria for clear peaks specified by SESAME (2004) were discarded.

3.3 Microzonation based on microtremor measurements

Microtremor surveys were conducted at 459 sites in Muscat region. Site responses that do not satisfy the reliability and stability criteria and the isolated ones were discarded, so that 306 microtremor surveys were finally used with the aim of assessing the fundamental resonance frequency (f_0) of the soft sedimentary cover in the study area. By spatial interpolation between these 306 microtremor measurements, a map of fundamental frequencies over the investigated area is obtained (Fig. 4). In addition, amplitude of the H/V spectral ratio curves at 36 sites is unaffected by any kind of site effect (flat curve) and experiences no significant amplification along the entire frequency band used in the current study. These H/V curves are indicative of non-weathered reference sites with minimal or no amplification even at high frequencies (e.g., Fig. 5). These typical hard rock sites are mostly concentrated in the eastern part of the study area and are located on the harzburgite and limestone formations. The locations of these typical rock sites are indicated on the map of resonance frequency by "F" letter (Fig. 4).

Many sites classified as hard rock at the eastern part of Muscat region show significant amplification at frequencies equal or higher than 10 Hz. Field observations and the boreholes data at these sites confirm the presence of thin weathered rocks overlying the hard rock suggesting that despite the broad geological classification as hard rock, locally the site conditions could vary depending on the presence or absence of weathered soil and its thickness.

Peaks around 1.5 and 6 Hz in some sites are noticed and proved to be of industrial origin. Some other industrial peaks were also reported around 16 Hz, but with less spatial extension than that at 1.5 and 6 Hz. It is also noted at very few sites in the eastern part of the investigated area that two peaks on the H/V curves were observed. These sites typically show a first maximum in the frequency range between 5 and 11 Hz, and a second one at frequencies higher than 15 Hz. One possible interpretation is that the low resonant frequency corresponds to the response of the relatively deep sediment layer, whereas the second peak could reveal the presence of a surficial layer with a high impedance contrast.

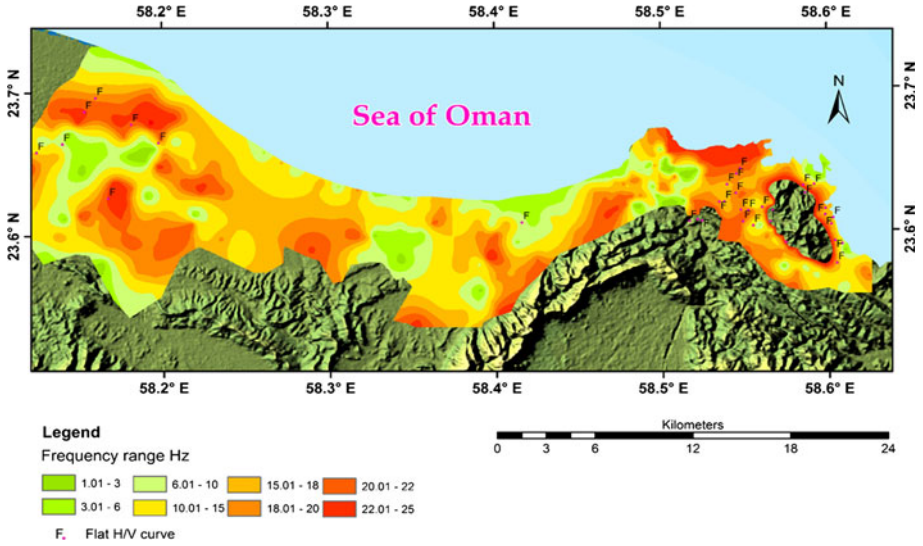

Fig. 4 Spatial distribution of the fundamental frequency using H/V spectral ratios results

This could not be an artifact induced by the seismometer, as we are in the flat part of the response curve of the sensor, which extend at least to 20 Hz.

The distribution map of f_0 shows that the resonance frequency varies within a short distance in Muscat (Fig. 4). This could be attributed to undulations in the bedrock, causing variations in soil thickness. The soil type also changes from place to place. In the eastern part of the region, the rocky outcrops of ophiolite and tertiary limestone are present, while Recent alluvium and depressions with Recent or sub-Recent clay and silt are present in the middle northern part. Analyzing the resulting map of resonance frequencies (Fig. 4), it is straightforward to identify the following general characteristics of the investigated area:

- Most of the region is dominated by high resonant frequency (equal to or greater than 10 Hz), which in consistency with the general geology of the region indicating that most of the area has a thin sedimentary cover or outcropping bedrock. These areas are concentrated mainly in the eastern, southern, and western parts of Muscat. Areas with smaller f_0 values (1.8–6 Hz) are observed at the coast line and wadis, where the thickness of the soft soil is relatively large.
- The middle and western areas are characterized by f_0 decreasing toward north direction from about 22 Hz to about 3 Hz;
- The westernmost area shows more irregular f_0 features, where the f_0 is about 3 Hz at the coast line; f_0 increases southward until at least 22 Hz, then decreases until 1.8 Hz, and finally increases again until about 22 Hz.

Comparison between the spatial distribution of the map of the resonance frequency and the surface geological map (Fig. 2) is very difficult, because at many sites in the area, the thickness of the Quaternary alluvium material which covered most of the western part of the study area is very thin as indicated by the available borehole data. For example, the relatively deep geotechnical borehole (Expway_8) taken in Muscat Expressway in Bawshar area (Fig. 6) appears on the geological map to lie on Aeolian sand, Recent or sub-Recent dunes and thus is apparently expected to have low f_0. The borehole Expway_8

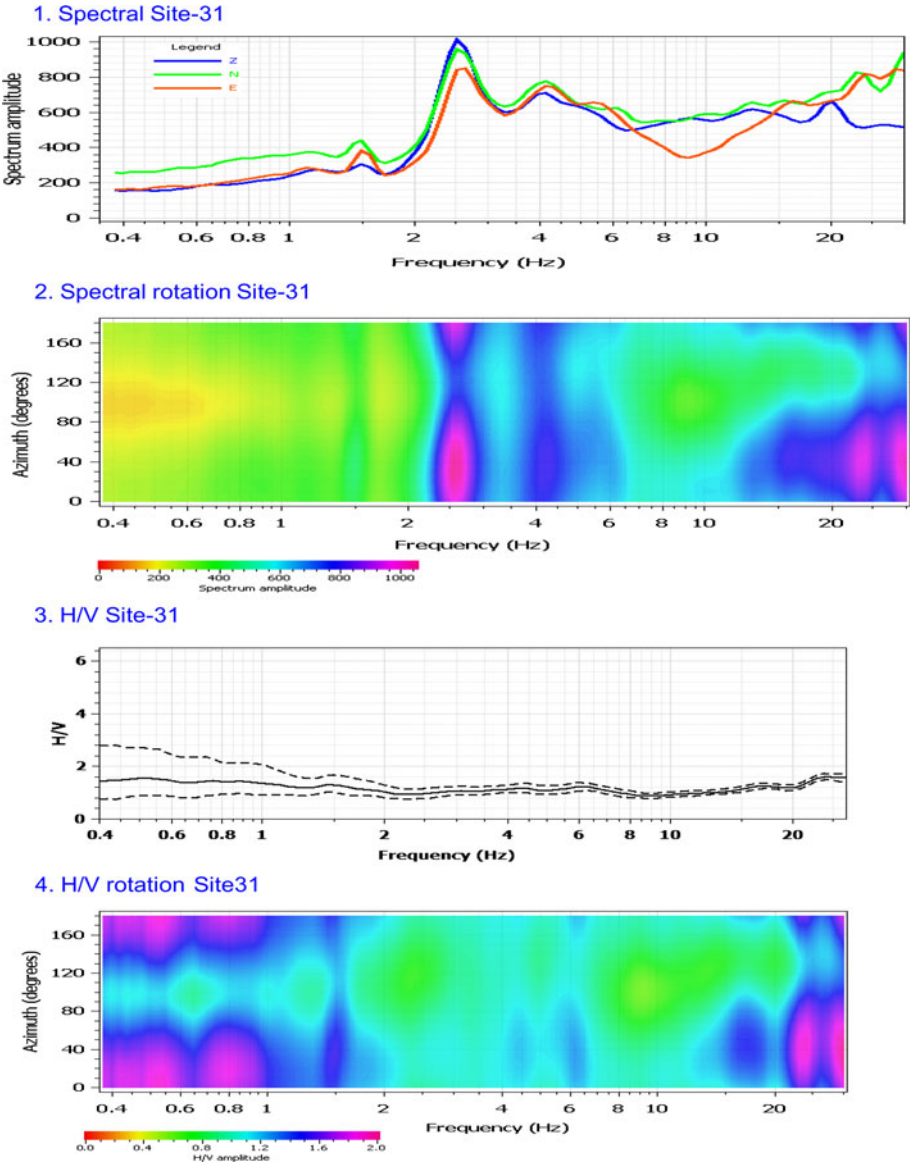

Fig. 5 *Panel 1* is the amplitude spectrum of three components at site-31, *Panel 2* shows the horizontal spectrum rotation with azimuth, *Panel 3* illustrates the H/V spectral ratio curve, and *Panel 4* shows the H/V rotation with azimuth

(Fig. 7) data show that the soft sedimentary cover is only 1.10 m thick, followed by hard limestone bedrock, and thus is actually characterized by relatively high f_0 ranging between 18 and 20 Hz (Fig. 4). Therefore, it is inappropriate to compare the f_0 values with the surface geology in the studied region. The f_0 limit of 10 Hz reproduces the outcropping ophiolite and limestone formations of the eastern part of the Muscat City.

The fundamental frequency distribution map could be interpreted taking into account both the height of a building and its fundamental frequency of vibration which can be expressed simply by the following approximate formula:

$$F = 10.0/(\text{number of stories}) \quad (2)$$

From this point of view, no resonance is expected to occur in most of the study area, which is characterized by fundamental resonance frequency equal to or greater than 10 Hz. The buildings, which would be most affected by site resonance when a destructive earthquake occurred, are located at parts of the coast area or inside some wadis, where the fundamental resonance frequency ranges between 2 and 6 Hz; these would be buildings of 2–5 stories. High-rise buildings of 5–12 stories have inconsistent resonance frequency with the fundamental frequency of the soil. No tall buildings (higher than 40 m) are allowed to be built in Muscat.

4 Evaluation of site response using SHAKE

Shear wave velocity (Vs) is the best indicator of stiffness (Bullen 1963; Aki and Richards 1980); therefore, it is recognized as a key factor in the site response of the soft soil (Borcherdt 1970). The amplification of ground motion is proportional to $1/(\mathrm{Vs}.\rho)^{0.5}$ where Vs is the shear wave velocity and ρ is the density of the investigated soil (Aki and Richards 1980). Since the change in density is relatively small with depth, the Vs value can be used to represent site conditions. Therefore, the shear wave velocity of the soil columns is used in the current study to define the amplification characteristics at carefully selected 99 sites (Fig. 8). These sites are selected so that all the surface geological units of the region of

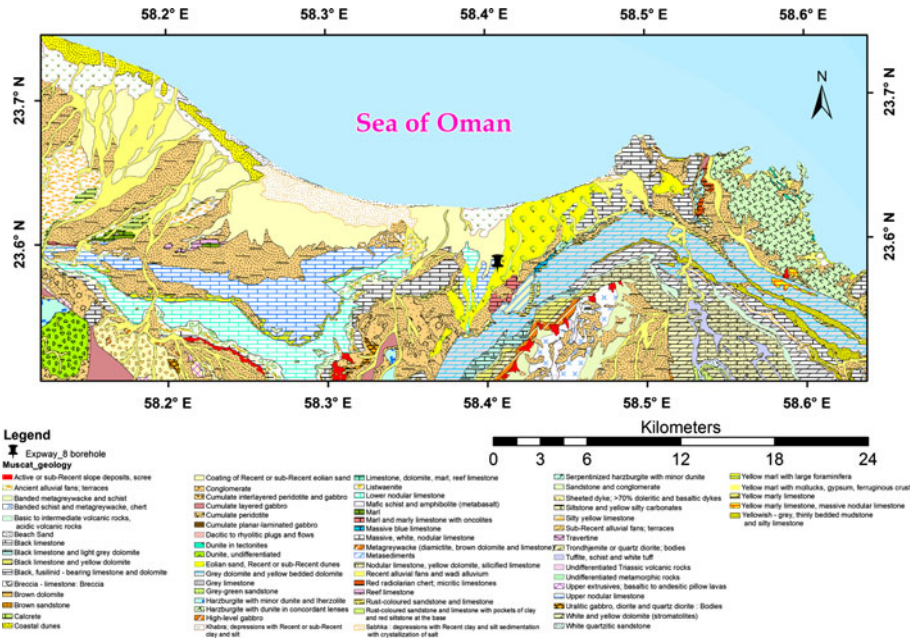

Fig. 6 Location of Expway_08 on the surface geologic map

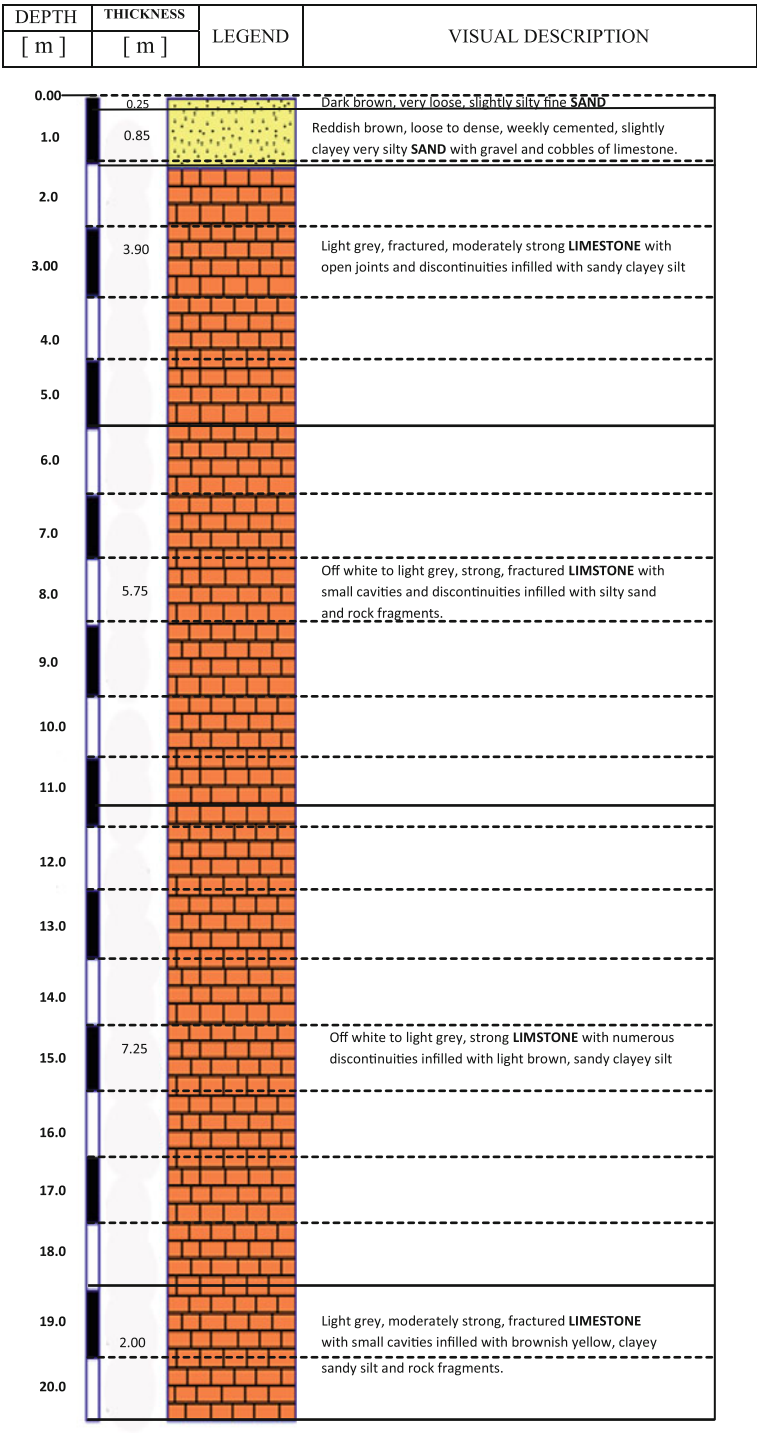

Fig. 7 Lithology of Expway_8 relatively deep borehole

interest are covered. Resultant shear wave velocity profiles are one of the most important inputs into SHAKE91 program.

S-wave velocity is derived by inverting the dispersive phase velocity of the surface Rayleigh wave utilizing the MASW technique (Park et al. 1999; Miller et al. 1999; Xia et al. 2000). This is done using SURFSEIS 3 software of Kansas Geologic Survey for the selected 99 sites. MASW is non-invasive, low-cost, rapid, robust, and moreover, it consistently provides reliable shear wave velocity profiles within the uppermost 30 m (Xia et al. 1999, 2000, 2002; Park et al. 1999; Tian et al. 2003; Mahajan et al. 2007; Seshunarayana et al. 2003; Seshunarayana and Sundarajan 2004). It generates 1-D Vs profile (i.e., Vs versus depth), and the 2-D shear wave velocity profile could be generated by interpolating the yielded 1-D ones. The MASW is successfully used in many studies (Xia et al. 1999, 2000, 2002; Park et al. 1999; Tian et al. 2003; Kanli et al. 2006; Anbazhagan and Sitharam 2008; Sundararajan and Seshunarayana 2011).

The inversion process for the dispersion curve of the Raleigh-type surface waves on a multichannel record requires an initial shear wave velocity profile, which is obtained in the current study using a conventional P-wave shallow seismic refraction measurement and a constant Poisson's ratio of 0.3 at each of the selected 99 sites of interest in order to convert the resultant P-wave velocity into initial Vs depth model. The resultant initial Vs depth models are used for the inversion process providing constraints for the shear wave model parameters improving thereby the reliability of the surface wave inversion process.

4.1 P-wave shallow seismic refraction data acquisition

The seismic refraction at the selected 99 sites was carried out through applying the forward, inline, mid-point, and reverse acquisition system to create the compressional waves

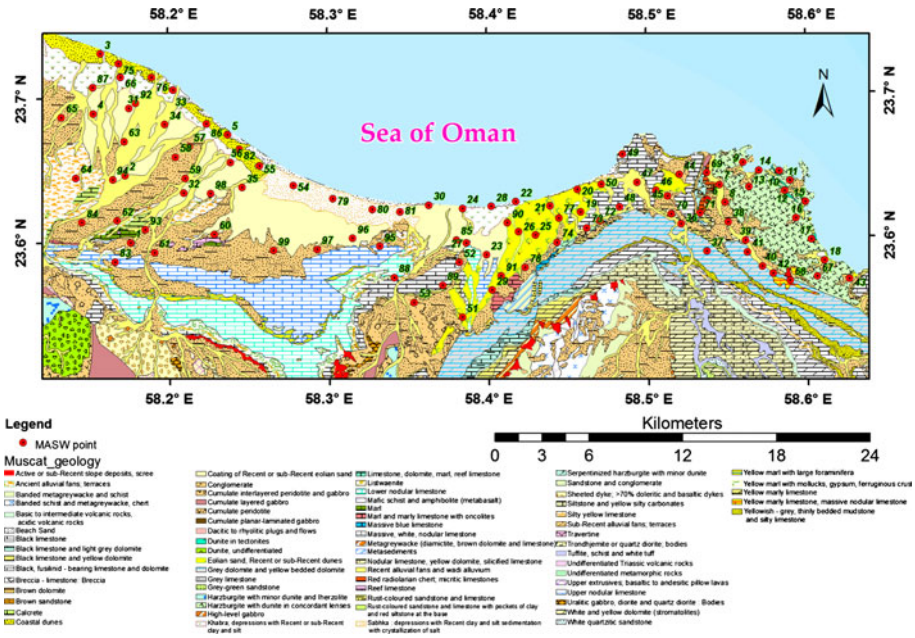

Fig. 8 Location of sites for shear wave velocity measurements on the surface geologic map of Muscat

(P-waves). The P-waves are acquired by generating seismic energy using a sledge hammer of 8 kg, sending the created seismic waves inside the earth. The direct and refracted waves are detected through 40 Hz vertical geophones. Most of the surveyed 99 profiles have 115 m long spread. Few seismic profiles have spread length less than 115 m data due to the unavailability of enough space at the target sites. The geophones, which were firmly coupled to the ground, had 5 m fixed geophone spacing. The technique is to shoot the profile (7 shots) at 25 m distance from both ends, 5 m distance from both ends, mid-point, in addition to 2 inline shots (between G6-7 and G18-19).

4.1.1 Shallow seismic data processing

The recorded P-wave data were first corrected to true elevation of each geophone and then processed and analyzed using the software supplied by Oyo (SEISREFA 1991). This software uses the ray tracing technique to interactively match the interpreted subsurface model to field data. The wave forms were analyzed by picking the first breaks (e.g. Fig. 9) and determining the travel time–distance (T-D) curves and depth models (e.g. Fig. 10).

4.1.2 Seismic interpretation

The deduced time distance curves and the corresponding 2-D depth model at each of the 99 profiles are obtained in order to interpret the subsurface features in terms of P-wave velocity. The agreement between the observed travel time curves and the calculated ray tracing at most of the sites indicates a good depth model results (e.g., Fig. 10). Many of the studied sites are located in urban settings where the original ground surface has been modified by the addition of artificial fill and/or one or more layers of engineered compacted soil and aggregate. These near-surface layers are seen in the raw seismic data as low-velocity direct arrivals and refracted phases. Shown in many of the velocity versus depth columns (e.g., Fig. 10) are one or two thin layers 1–3 m thick with relatively low velocity.

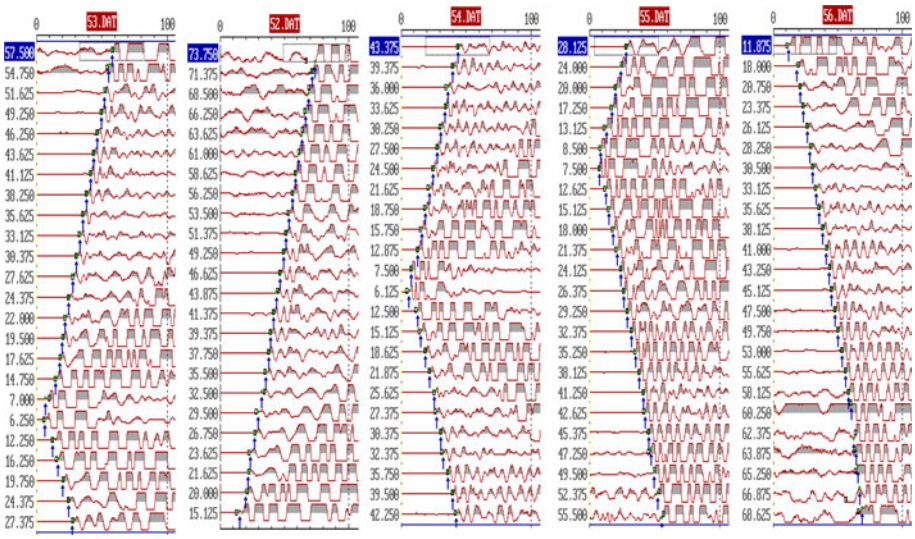

Fig. 9 Picking of the first arrival at five out of seven seismograms at site no. 20

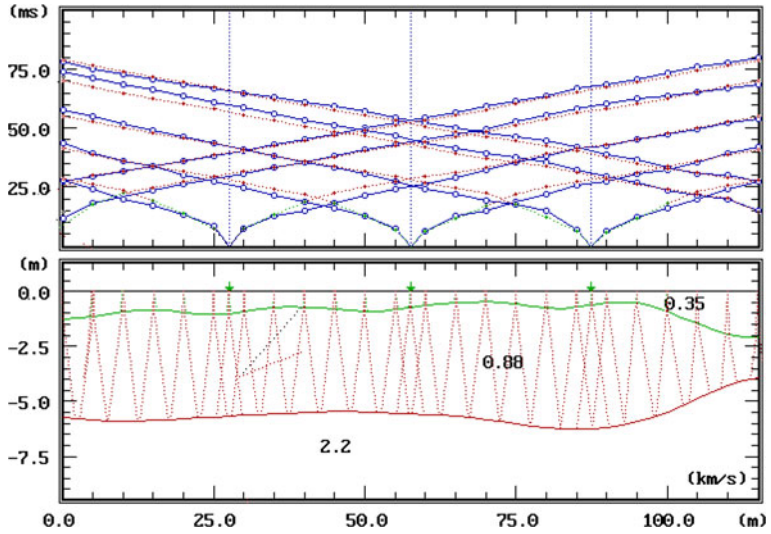

Fig. 10 Travel time–distance curves and depth model at site no. 20

Generally, in the western part of the study region, the obtained subsurface layers consist mainly of three layers. The first layer with a thickness of 1–4 m is formed mainly from filling and sands with P-wave velocity varying from 300 to 600 m/s. The second layer with a thickness of 3–10 m is made up of sands and gravels with medium physical properties (P-wave velocity ranges between 800 and 1,200 m/s). The P-wave velocities of the third layer which consists usually of hard rock (limestone) ranged between 1,500 and 2,700 m/s. A typical example of such depth models is shown in Fig. 10.

In the eastern part of the study area, the area is characterized mainly by three layers. The first layer has velocity ranges from 500 to 900 m/s and a thickness of about 2–4 m. The second layer has velocity range from 1,200 to 1,500 m/s and thickness of about 6–12 m, while the third layer has a velocity range from 2,400 to 4,500 m/s. Figure 11 shows a typical example of such interpretation. Available shallow geotechnical boreholes (up to 10 m depth) reveal that the first layer in some cases could be weathered rock underlain by the bedrock, which could be ophiolite or dolomitized limestone. Other boreholes show that sand followed by gravel or mixture of them are extended to the bottom of the shallow borehole or underlain by the weathered rock and ophiolite.

4.2 MASW data acquisition

In the current study, a 24-channel signal enhancement seismograph "StrataView" of Geometrics Inc., USA, was employed for data acquisition along the selected 99 sites (Fig. 8). The main task was to estimate the shear wave velocity of subsurface layers as deep as possible, so the frequency content of the records had to be low enough to obtain phase velocities at longer wavelengths, which results in a larger depth of investigation. Therefore, 4.5 Hz geophones, which record the lower-frequency components effectively, were used. Recording sampling interval of 1.0 ms and recording length of 1,024 ms were applied.

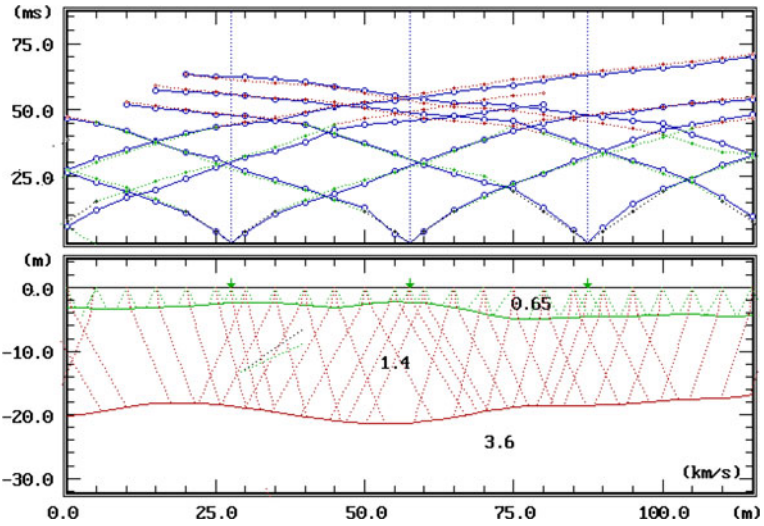

Fig. 11 Travel time–distance curves and depth model at site no. 51

The most important parts of the field configurations are the geophone spacing and the offset range. The planar characteristics of surface waves evolve only after a distance greater than the half of the maximum desired wavelength (Stokoe et al. 1994). The acquisition layout was an array of vertical sensors with 1 m geophone spacing and 4 m shot interval. Based upon the field observations, the source to nearest receiver offset was changing between 5 and 10 m. The energy source was an 8-kg sledge hammer all through the survey. Standard roll-along technique was used to achieve a continuous shot gather over a line spread of 52 m.

4.2.1 MASW data processing

The shot gather data require the following pre-processing:

1. The conversion of the raw seismic data format (SEG-2) into Kansas Geological Survey data processing format (KGS), combining all shot gathers for processing into a single file. Field geometry was assigned and acquired data were recompiled into the roll-along mode data set.
2. Pre-processing data inspection for the removal of bad records/traces.
3. There are several factors that interfere and disturb analysis, body waves, and higher mode surface waves. These noise sources can be partially controlled during data acquisition, but cannot be eliminated totally. This noise needs to be identified and eliminated through filtration and muting.
4. Preliminary processing to assess the optimum ranges of frequency and phase velocity.

After analyzing the overtone image of each shot gather, which represents the phase frequency versus phase velocity, phase velocity and phase frequency could be assigned for dispersion analysis. The fundamental mode of the surface wave is the input signal used for the current analysis. Accurate Vs solely depends on the generation of a high-quality dispersion curve, which is one of the most critical steps because the dispersion curve has

the greatest influence on the confidence in the Vs profile. The dispersion curve with the highest signal-to-noise ratio (S/N) represents the best choice (e.g., Fig. 12).

Each dispersion curve is individually inverted to generate a 1-D shear wave velocity profile using SurfSeis 3 software. The inversion process aims at finding a Vs profile whose theoretical dispersion curve matches with the experimental dispersion curve obtained from dispersion analysis. The match is evaluated on the root–mean square error (RMSE) between the two curves. The inversion algorithm first calculates the theoretical curve using the initial Vs profile and then compares theoretical curve with the experimental curve. If the RMSE is greater than the minimum RMSE ($E_{\min}$) specified in the control parameters, the inversion algorithm modifies the Vs profile and repeats the procedure by calculating a new theoretical curve. These iterations continue until either $E_{\min}$ or maximum number of iterations (Imax) is reached. These 1-D profiles appear to be most representative of the material directly below the middle of a geophone spread (e.g., Fig. 13).

The generated 1-D plots of shear wave velocity profiles have been interpolated in order to produce 2-D shear wave velocity profiles at each site (e.g., Fig. 14). The low RMSE in estimating the Vs at most sites suggests a high level of confidence (e.g., Fig. 15). The RMSE is a measure of relative error for each layer in comparison with theoretical criteria and can be used as a measure of confidence (Xia et al. 1999). In our analysis, the observed phase velocity at lower frequencies (e.g., Fig. 16) made it feasible to obtain information down to depth of 30–40 m for most sites.

Few boreholes with depth greater than 10 m are available in the study area (Fig. 17). Most of them are located on the shore line and conducted to repair As-Seeb Cornish road. It was not possible to conduct any MASW survey on these boreholes due to inaccessibility. Fortunately, it was possible to conduct some MASW measurements in the south part of the

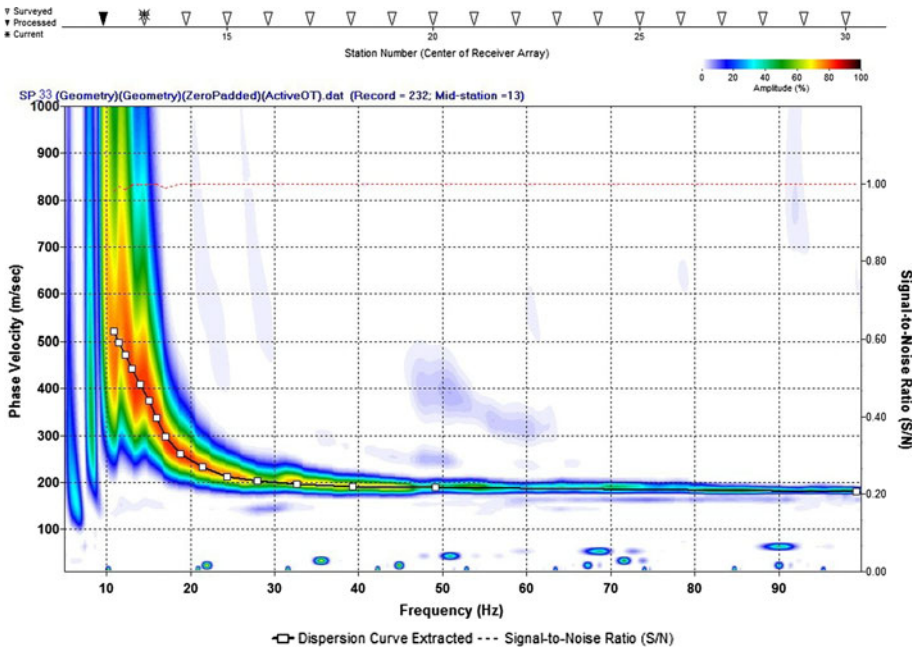

Fig. 12 The dispersion curve with overtone image for site no. 33

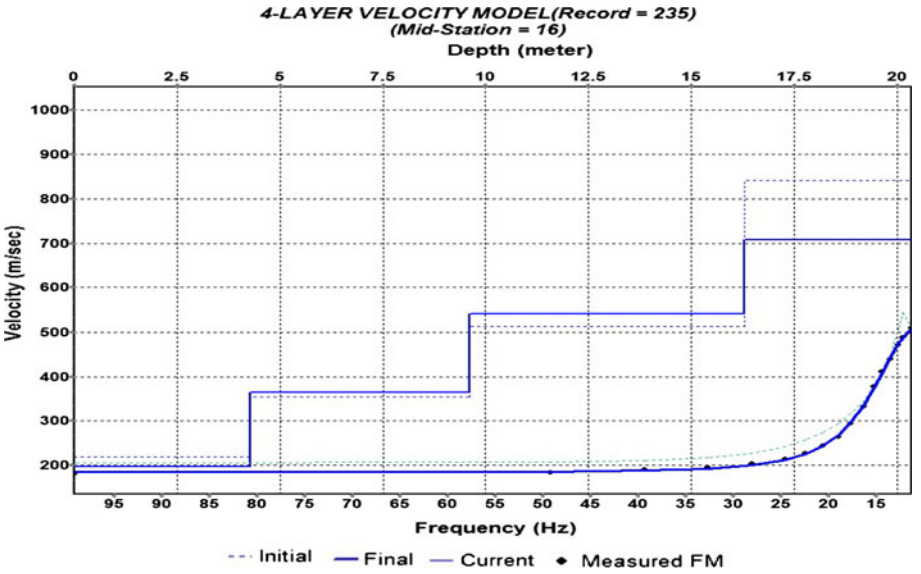

Fig. 13 1-D velocity-depth inversion at site no. 33

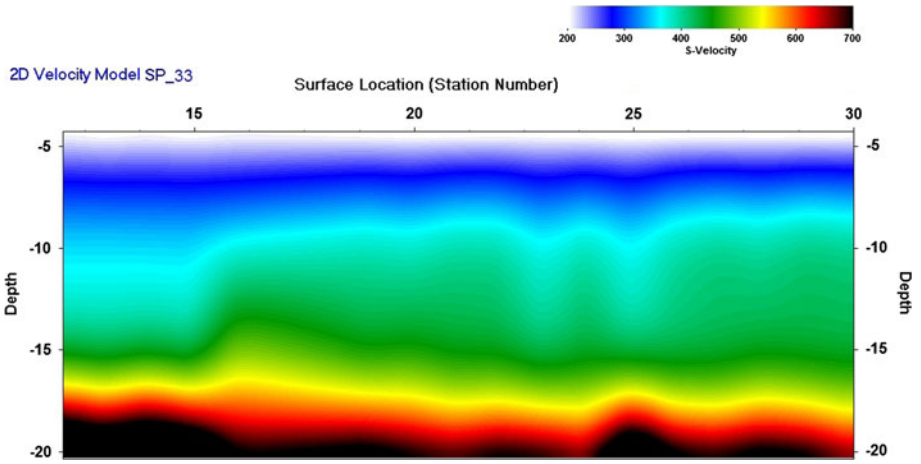

Fig. 14 2-D velocity model for site no. 33

study area at the geotechnical boreholes of the Muscat Express way. A good agreement in terms of thickness and shear wave velocity variation is observed between the MASW results and the borehole data (Fig. 18).

The V_{S30} values were calculated from shear wave velocity profiles and transformed into site classification based upon the NEHRP (2001) guidelines (Fig. 19). Most of the region belongs to the *C* category ($360 \leq V_{S30} \leq 760$ m/s). There are also considerable parts of the region which are located on the rocky eastern, western, and southern areas and have better soil conditions corresponding to B class ($760 \leq V_{S30} \leq 1{,}500$ m/s). Only two sites at the northern middle coast belong to D category ($180 \geq V_{S30} \geq 360$ m/s). These two

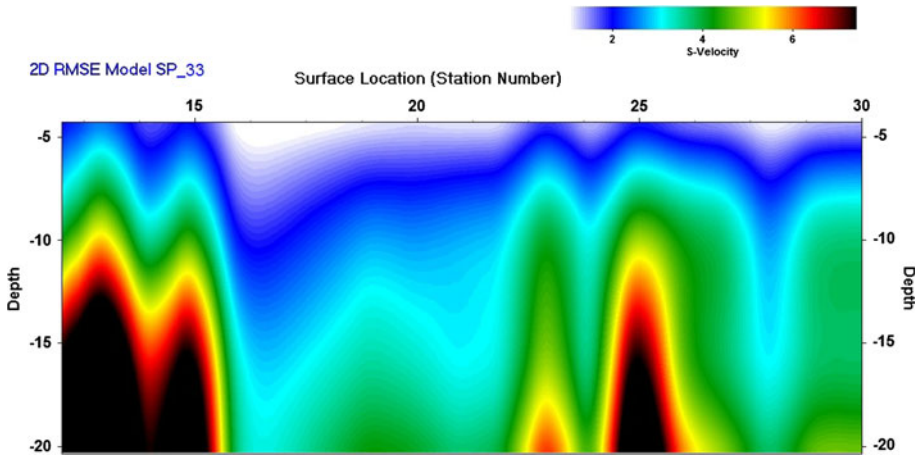

Fig. 15 2-D RMSE model for site no. 33

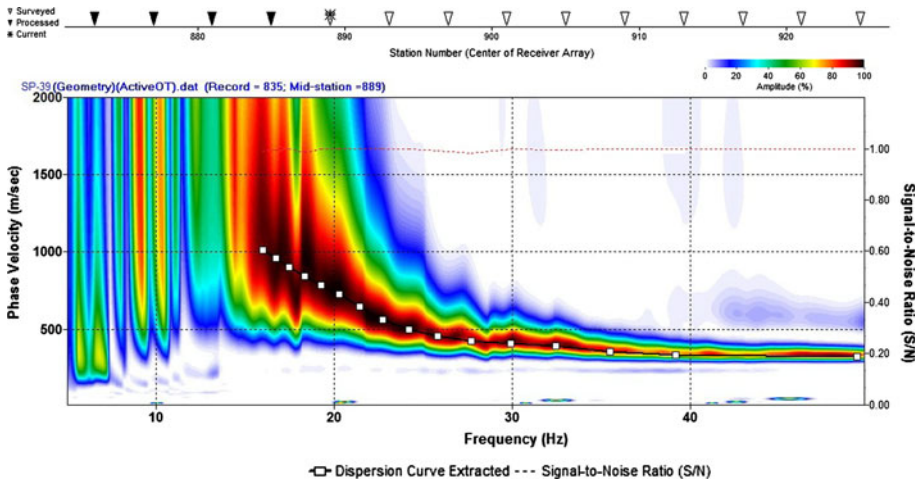

Fig. 16 The dispersion curve with overtone image for site no. 39

sites are associated with the presence of depressions with Recent or sub-Recent clay and silt and Aeolian sand (Fig. 2). In these sites, the V_{S30} values are close to the lower limit of NEHRP class C. The results show that the depth of the engineering bedrock (Vs $\geq$ 750 m/s) in most sites is less than 30 m, the depth that reached for most sites using the MASW method.

4.3 1-D ground response analysis using SHAKE91

As described by Kramer (1996), soil response to the strong ground motion can be approximated by the transfer function of layered and damped soil on elastic rock. The methods of 1-D ground response analysis are useful for level or gently sloping sites with parallel material boundaries. Such conditions are common and one-dimensional analyses are widely used in geotechnical earthquake practice (Kramer 1995).

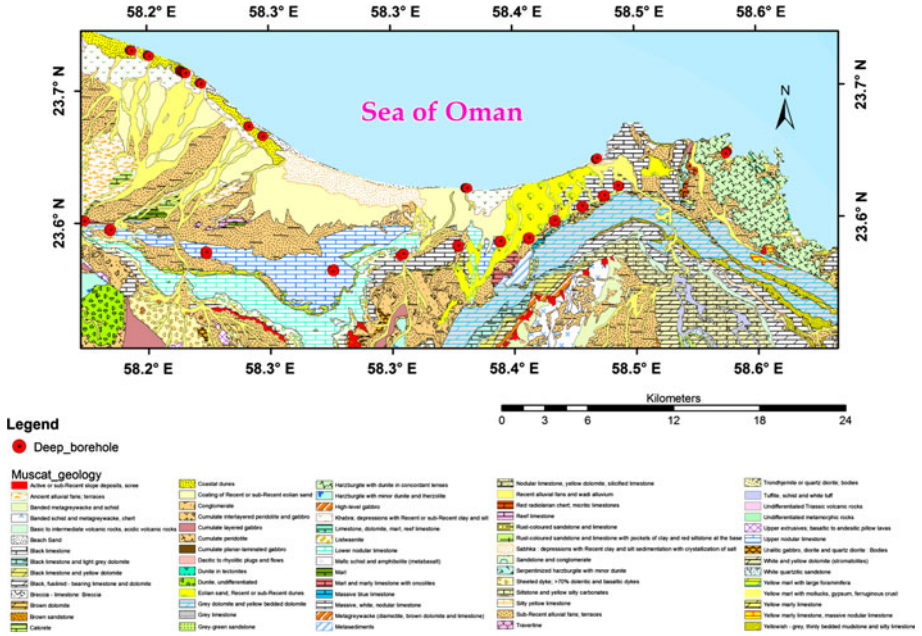

Fig. 17 Location of relatively deep boreholes (up to 25 m depth)

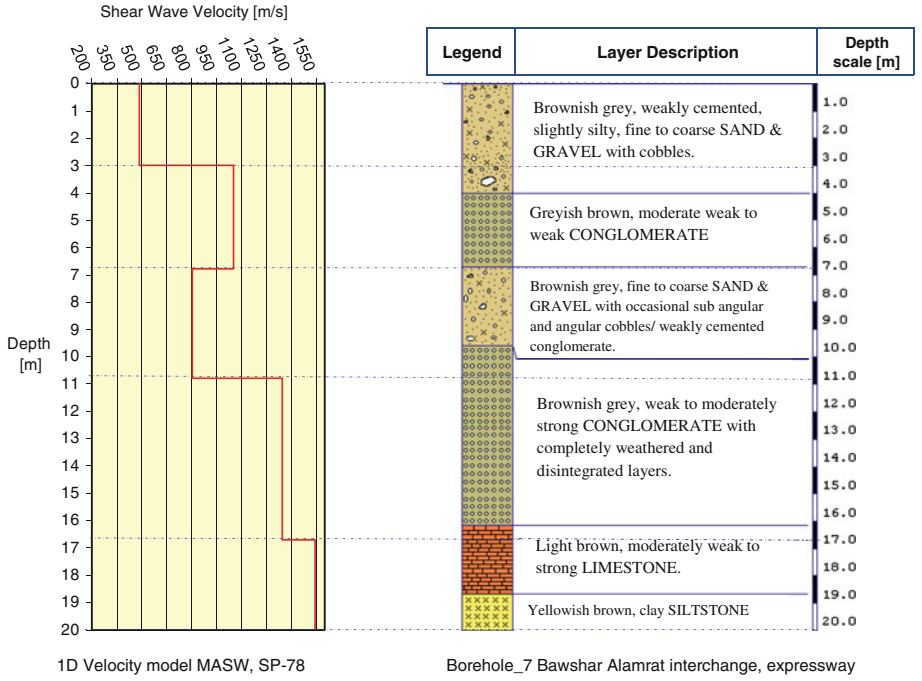

Fig. 18 Correlation between 1-D MASW velocity model at site no. 78 and borehole_7 Bawshar Al-Amerat interchange, Muscat Express Way

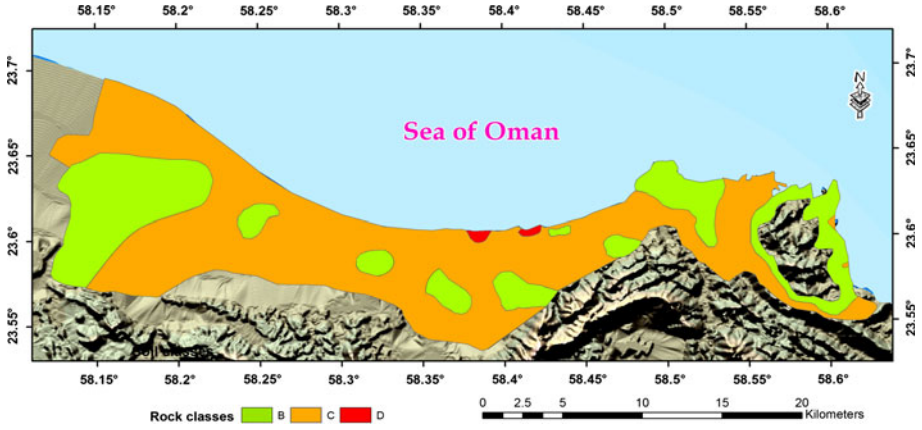

Fig. 19 Site classes map across Muscat region according to NEHRP site classification

The earliest and most widely used software written that uses this principle is called SHAKE. The computer program SHAKE was written in 1970–1971 by Dr. Per Schnabel and Prof. John Lysmer (Schnabel et al. 1972). SHAKE was modified and became SHAKE91 (Idriss and Sun 1992) with an equivalent linear approach for the nonlinear response. SHAKE91 was used to characterize the amplification factors and associated characteristic site periods and to map ground motion hazards in many metropolitan areas around the world (e.g., Street et al. 1997, 2001; Cramer et al. 2004, 2006).

4.3.1 Input data for the ground response analysis

The most important input information for the ground response analysis is a subsurface model that represents the variation with depth of the soil layers. Subsurface profile information, thickness, shear wave velocity, density, and lithology are obtained from MASW results and the information of the available boreholes. This information is compiled for the selected 99 sites and used for the 1-D response analyses using SHAKE91 program in EZ-FRISK7.62 software.

The nonlinear behavior of soils is well known and can be determined very well in a laboratory environment. Shear strength reduces with shear strain, while damping increases with shear strain. These relationships can be tested and plotted in curves, called shear modulus reduction curves and damping curves. A soil property of each layer is modeled by using modulus reduction (G/Gmax) and damping (ξ) versus shear strain curves. The degradation curves for sand, gravel, and rock used for the present work are those proposed by Seed and Idriss (1970), Seed et al. (1986), and Schnabel et al. (1972), respectively.

4.3.2 Earthquake input for the site response analyses

One of the basic problems associated with the study of seismic microzonation is to determine the seismic ground motion, at a given site, due to an earthquake with a given magnitude (or moment) and epicentral distance. The ideal solution for such a problem is to use the local wide database of real recorded strong motions and to group those accelerograms that have similar source, path, and site effects. The use of real earthquake accelerograms carries reassuring knowledge that the input motion is a genuine record of shaking

actually produced by an earthquake. Including parameters such as amplitude, frequency and energy content, duration, and phase characteristics, the real accelerograms reflect the influence of many characteristics of the source, path, and site that influence the nature of strong ground motion.

Due to the lack of strong motion data in the Muscat region and in Oman as a whole, the authors preferred to use ground motion records from the international strong ground motion databases. EZ-FRISK 7.62 was used in order to search in the accelerogram databases to define the real earthquakes that best compatible with the PSHA results. The deaggregation of seismic hazard for Muscat area is used to determine the controlling earthquake scenarios in terms of magnitude and distance. Moderate magnitude earthquakes have the largest contribution for the short-period seismic hazard, while large-distant events (180–210 km) have the largest contribution to the seismic hazard at longer periods (Fig. 20).

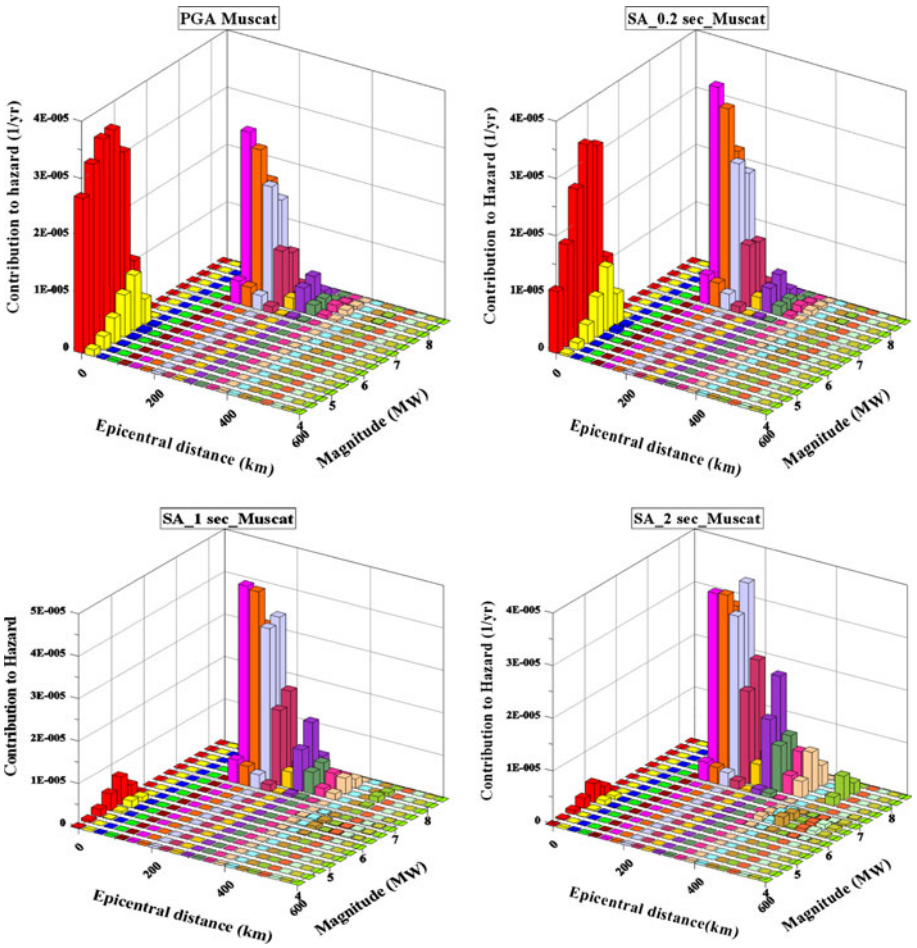

Fig. 20 Deaggregation results showing the relative contribution to the PGA and spectral accelerations of 0.2, 1.0, and 2.0 s as a function of magnitude and distance at rock site in Muscat City for return period of 2,475 years

The best time history database available for use with EZ-FRISK at the time of conducting this study was the PEER NGA7.3 database. This data set is primarily for tectonically active regions. For tectonically stable regions, the USNRC CEUS database is available. It contains 921 earthquake strong motion records. The majority of the records, 882, are for events in tectonically active regions that have been adjusted to be representative of events in the United States stable regions.

The selected records are then modified using the spectral matching technique in order to compensate for the inevitable mismatch between their characteristics and the design parameters established from the site-specific hazard assessment. EZ-FRISK7.62 uses the well-known RspMatch2009 spectral matching algorithm with modifications to preserve non-stationarity at long periods by using different functional forms for the adjustment time history (Al Atik and Abrahamson 2010).

Distance and magnitude of earthquakes with the largest contribution to the earthquake hazard were used to search the available databases. The duration is suggested to be 20 s for the short-period events and 80 s for the large-distant events. The input acceleration time histories were matched with the unified hazard spectra (UHS) of Muscat region for 475 years return periods obtained from earthquake hazard study (Fig. 21) using Al Atik and Abrahamson (2010) approach. The matched accelerograms were then used as input for site response analyses (SHAKE91), and the average of the calculated amplifications, PGA, and spectral accelerations were calculated for each of the selected 99 sites to obtain the necessary parameters for microzonation.

The amplification curve at site (20) is an example of a single curve of 4.2 amplification occurred at 13.1 Hz. This 13.1 Hz is the fundamental frequency as indicated also by the results of H/V spectral ratio analyses at the same site (Fig. 22). The amplification curve shown in Fig. 23 presents two peaks at site 90, the first peak with amplification of 2.4 occurred at 6.25 Hz and the second peak of 1.6 amplification value occurred at 18.8 Hz. In the amplification spectrum, the maximum amplification ratio occurred at 6.25 frequency, which is the fundamental frequency of the soil column in that location. This is confirmed also by the results of H/V spectral ratio analyses (Fig. 23). Amplification curves with two and multiple peaks were identified at few sites in the area of study. Results clearly show that with exception of very few sites, the fundamental frequencies obtained using the H/V technique and those obtained using SHAKE91 technique are well matched.

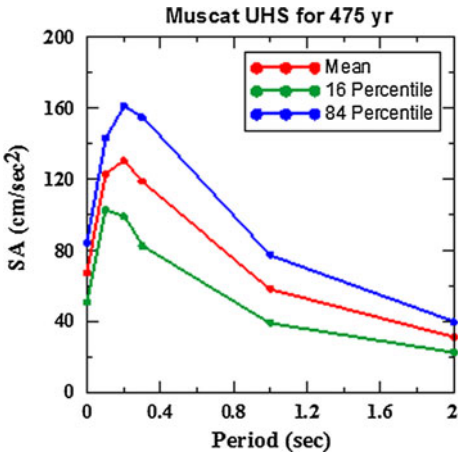

Fig. 21 Mean, 16 percentile, and 84 percentile UHS for rock sites in Muscat City for the 475 years return period

4.3.3 Amplification maps

The delineation of high seismic vulnerability regions can be made by identifying regions susceptible to higher amplification of the bedrock motion. The term amplification curves are used here to refer to the ratio of the spectral ground motion at the ground surface to that at the bedrock. These curves are evaluated for all the selected 99 sites using the shear wave velocity–depth models derived by MASW method and the input ground motion records.

Most of the amplification factors thus calculated for the PGA values for 475 years return period range from 1.0 to 2.0 (Fig. 24). It is very clear that B and C class regions with V_{S30} close to the border of B class on NEHRP classification almost have no PGA amplification. The maximum PGA amplification value for such regions is 1.25. Regions of Muscat can be divided into three zones based on the range of PGA amplification factors assigned to each zone. The eastern and western parts experience no PGA amplification, the middle northern part with PGA amplification in the range between 1.5 and 2.0, and the middle southern part, which is characterized with PGA amplification factors less than 1.5.

The amplification functions for 475 years return periods derived between free surface and the bedrock show that the map of highest amplification factors is the 0.1 s spectral period (Fig. 25). The amplification factors at spectral periods of 0.1 s range from 1.0 to 4.4. The upper bound value of this range is observed only at one site of D class on NEHRP classification on the middle northern cost of Muscat. Most of the amplification factors calculated at spectral period of 0.2 s range between 1 and 2.8. One site only at the western side of northern coast of Muscat has an amplification factor of 3.46 (Fig. 26).

The amplification map at spectral period of 0.3 s is very important since most of the buildings in Muscat region have natural frequency similar or very close to this period. The amplification factors at 0.3 spectral period range from 1.0 to 2.75. Most of the study area is characterized by amplification factors less than 1.5 (Fig. 27). The amplification factors at

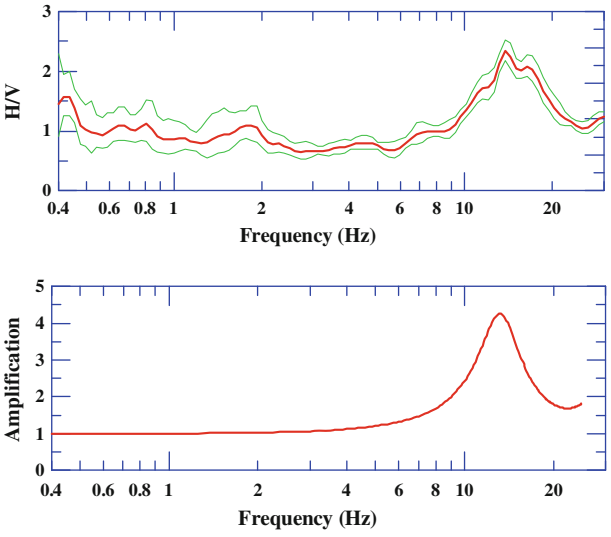

Fig. 22 Correlation between the fundamental resonance frequency obtained by H/V spectral ratio (*upper graph*) and SHAKE91 (*lower graph*) at site no. 20

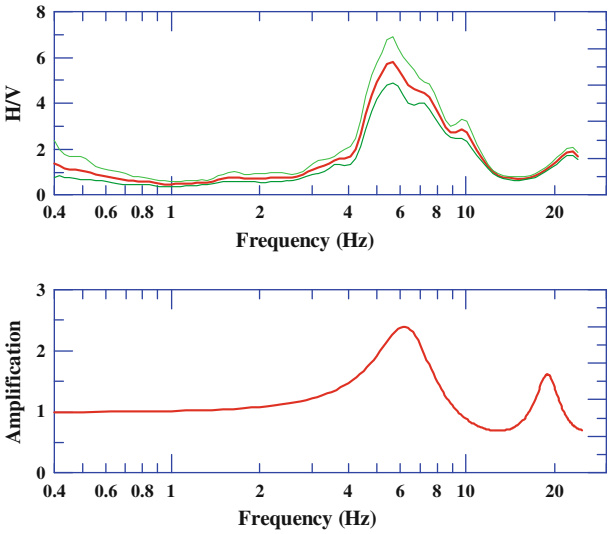

Fig. 23 Correlation between the fundamental resonance frequency obtained by H/V spectral ratio (*upper graph*) and SHAKE91 (*lower graph*) at site no. 90

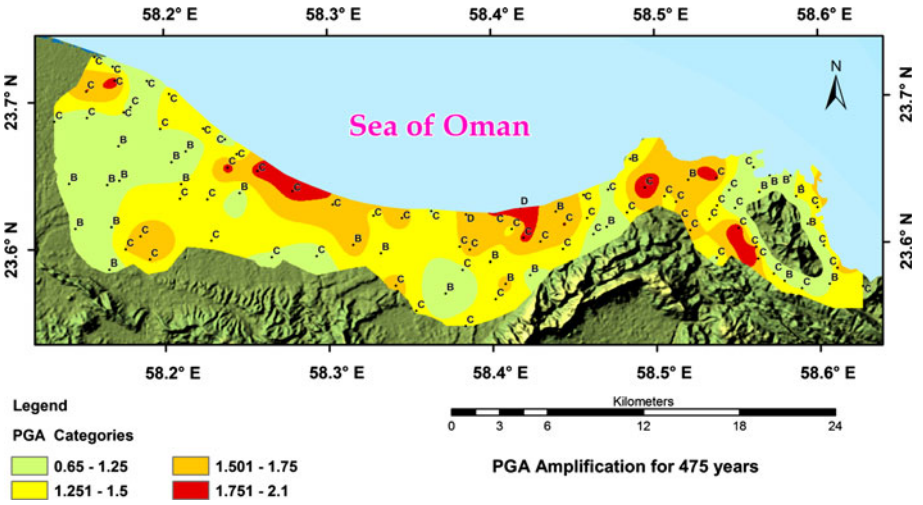

Fig. 24 Microzonation map based upon the PGA Amplification in Muscat for 475 years return period input ground motion

1.0 and 2.0 s spectral periods show almost no amplification at the region of interest. Therefore, no resonance is expected due to the soil effect for the high-rise buildings.

4.3.4 Surface ground motion maps

Selected results only are presented herein; the complete surface ground motion maps for a range of frequencies and return periods are available in (El-Hussain et al. 2012b). The earthquake response spectrum at the surface for each site has been derived using SHAKE91 software for damping level of 5 % of the critical damping for ground motion of 10 %, chance of exceedance in 50 years. The PGA and 5 % damped spectral acceleration

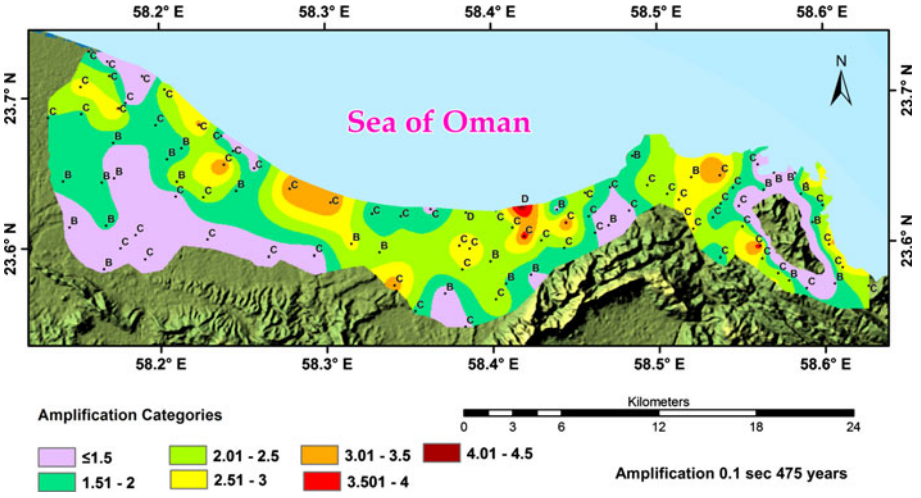

Fig. 25 Microzonation map based upon the 0.1 s amplification in Muscat for 475 years return period input ground motion

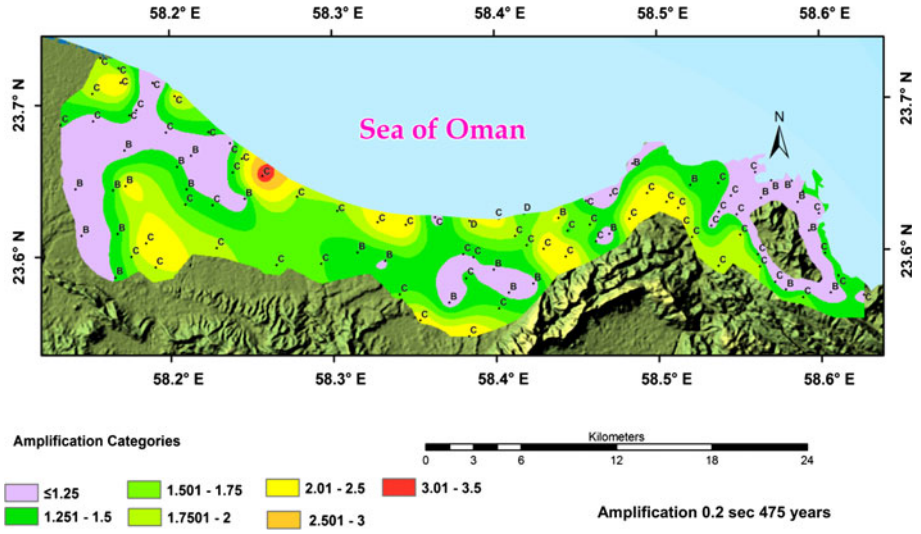

Fig. 26 Microzonation map based upon the 0.2 s amplification in Muscat for 475 years return period input ground motion

values spectral periods were mapped using ArcGIS10 by interpolating the ground motion values at the surface of the selected 99 sites. Therefore, the spectral acceleration of important range of spectral periods for common engineered structures in Muscat is covered in these maps.

The ground surface seismic hazard maps at the surface delineate the eastern and western regions of lower hazard from the remaining area. The PGA obtained at the ground surface in Muscat region ranges from 0.059 to 0.145 g for return period of 475 years (Fig. 28). The

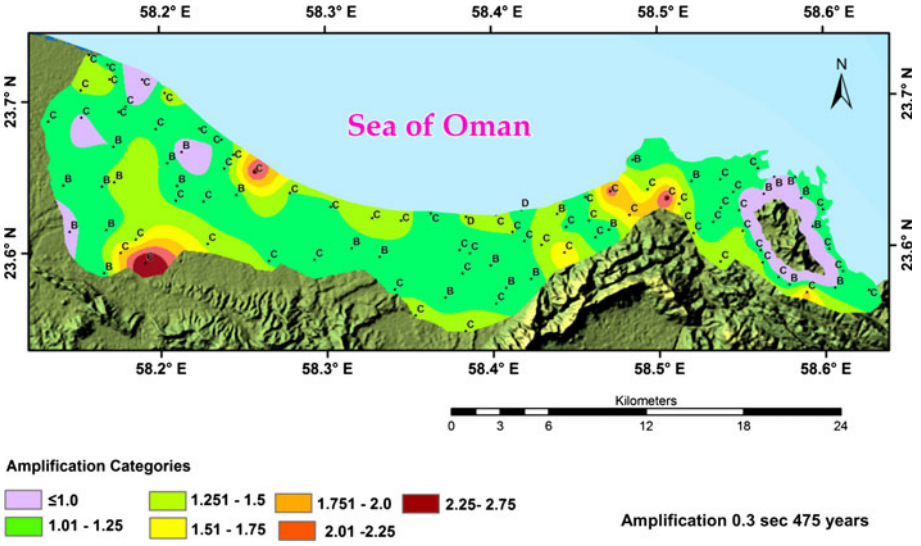

Fig. 27 Microzonation map based upon the 0.3 s amplification in Muscat for 475 years return period input ground motion

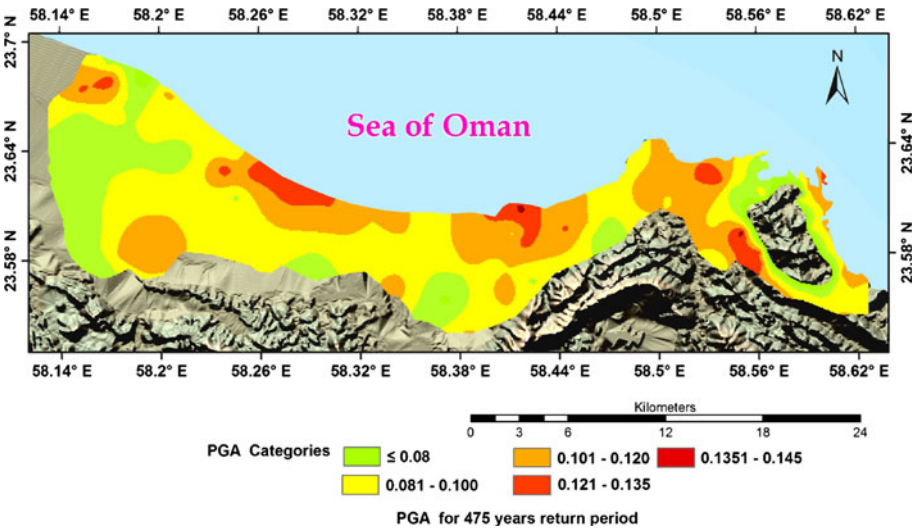

Fig. 28 Seismic microzonation for Muscat region in terms of ground surface PGA in g for 475 years return period

southern parts of the study area have a low level of seismic hazard due to its proximity from the rocky area of Oman Mountains with minimal soil effect on the ground motion.

Among the mapped spectral periods, the maximum surface ground motion values are associated with the 5 % damped horizontal spectral acceleration at a period of 0.1 s (equivalent to natural frequency of one story houses), where the maximum ground motions reach 0.47 g for 475 years return period at two areas in the northern middle part of the

study area (Fig. 29). Apart from these two sites, the maximum ground motion in the study area for 5 % damped horizontal spectral acceleration with a period of 0.1 s is 0.4 g for 475 years return period. The calculated accelerations for even larger houses are lower than those for the 0.1 s buildings. The spectral acceleration for two-story buildings (5 Hz natural frequency) shows the acceleration value in the range of 0.08–0.46 g for 475 years return period. The surface ground motion in the study area for 5 % damped horizontal spectral acceleration with a period of 0.3 s ranges from 0.11 to 0.35 g for 475 years return period (Fig. 30).

Plots of the surface hazard maps of 1 and 2 s spectral periods are normally much lower and less concentrated than the ones for higher frequencies at 0.1 and 0.2 s. These spectral accelerations are very close to those at the bedrock with no serious amplifications. Therefore, the variation of spectral accelerations at 1.0 and 2.0 s for 475 years return period is very small along the entire region of study. This analysis corresponds with the general conclusion that mainly the low-rise buildings may be resonated if an earthquake occurred nearby Muscat while high-rise buildings are expected to be of much less resonance than the shorter ones.

5 Discussion

The fundamental frequency map allows identifying which buildings in this area could suffer more damages due to coincidence of the fundamental frequency of the soil and the fundamental frequency of vibration of the building. According to the fundamental resonance frequency distribution maps, short buildings at the area may suffer more when a destructive earthquake occurs at the surrounding region, while the high-rise ones will be more stable.

It is inappropriate to compare the fundamental frequencies with the surface geology in the studied region. In many sites in the area, the thickness of the recent alluvium material

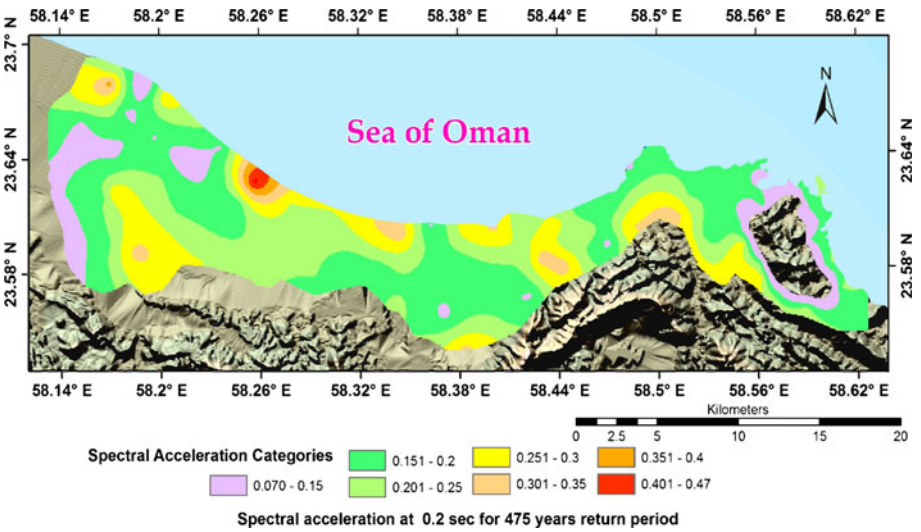

Fig. 29 Seismic microzonation for Muscat in terms of ground surface 0.1 s spectral acceleration in g for 475 years return period

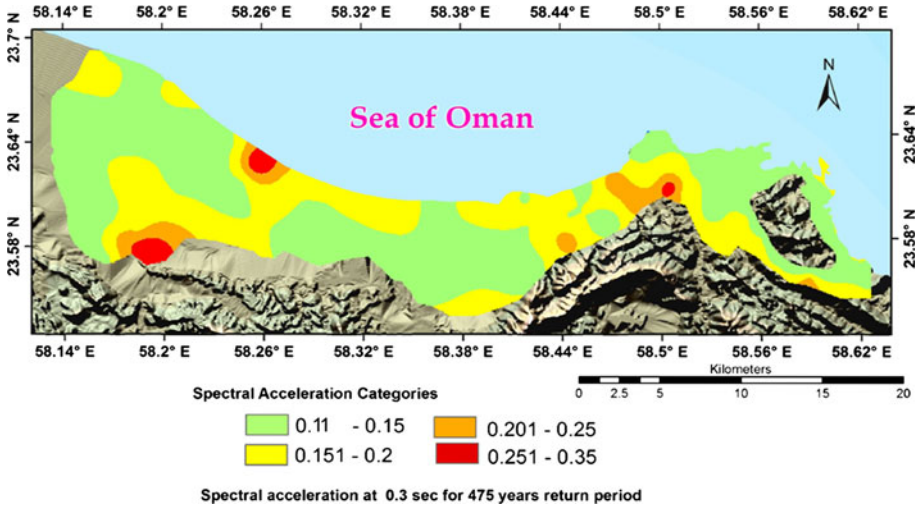

Fig. 30 Seismic microzonation for Muscat in terms of ground surface 0.3 s spectral acceleration in g for 475 years return period

which covered most of the middle and western parts of the study area is very thin as indicated by the borehole data. Therefore, these areas reflect fundamental site characteristics comparable with the hard material sites.

Several areas of the region of interest classified B type on NEHRP are covered with variable thicknesses of recent deposits or weathered rock, which has the potential to amplify the ground motion. The highest amplification is thought to associate with the depressions with Recent and sub-Recent silt and clay in the middle northern parts of the study area. Thus, significant amplification is expected at these sites of soft soil, while the remaining regions show lower amplification.

The amplification factors at B class on NEHRP classification is very low and even negligible at most of the investigated spectral periods, while sites on D and lower range of C classes on NEHRP classification show larger amplification. At most sites and for all the investigated periods, the amplification factor is less than 2.0.

The ground surface response spectra with 5 % critical damping value were calculated using shear wave profiles of MASW results and modified earthquake time histories by the spectral matching technique. The spectral acceleration values for all the locations at PGA, 0.1, 0.2, 0.3, 1.0, and 2.0 s are computed. The above spectral periods from 0.1 to 2.0 s were selected as they represent the range of natural periods of about 20 story's buildings to single story buildings. This range is enough to cover all the building heights in Muscat.

Although the response spectra for all the selected 99 sites are available, the contour maps presented here allow an engineer to construct an approximate response spectrum for the design purposes for sites in Muscat. These response spectra could now reflect an approximate surface ground shaking at each period.

The zones shown on the hazard maps should not serve as a substitute for site-specific evaluations at the critical and very important sites based on subsurface information gathered at such sites.

It is very important to recognize the limitations of these hazard maps, which do not include information with regard to the probability of damage. Rather, they show that when

strong ground shaking occurs, damage is more likely to occur, and be more severe, in the higher hazard areas. However, the higher hazard areas should not necessarily be viewed as unsafe. Therefore, data on the vulnerability of buildings, population, critical facilities, etc., should be gathered to provide risk maps of Muscat.

6 Conclusion

This paper constitutes the first attempt for microzonation in Muscat region. It provides fundamental resonance frequency map, amplification maps, and the ground surface seismic hazard maps. Microtremors measurements were carried out at 459 sites in Muscat region in order to map the fundamental resonance frequency and to identify areas prone to site amplification in the region of interest. The map of fundamental resonance frequency shows an increase from about 3.0 Hz in the north to 23.0 Hz in the south. Sites at the eastern and western parts of the study area have flat H/V curves around the unity or high fundamental resonance frequency peaks indicating rocky sites or sites covered with very thin soft soil. The lowest fundamental resonance frequency is at the middle northern coast, where a thickness of sedimentary cover is present.

Furthermore, 2-D MASW measurements were performed at 99 sites in the area of interest with the aim of the estimation of the shear wave velocity profile and the identification of the presence of strong impedance contrast responsible of seismic ground motion amplification. MASW results are compared to the data of boreholes of more than 10 m depth logged in Muscat Express Way and good agreement between the shear wave velocity profile and the lithologic column is indicated. Unfortunately, the borehole data were sparse and the study team could not make additional comparisons to come with conclusive statements about the efficiency of MASW technique to define the lithologic column in the region of interest.

Using the calculated shear wave velocities, SHAKE 91 modeling software, the responses were calculated. The SHAKE 91 calculations have been carried out for 99 sites where shear wave velocity profiles have been obtained. For input events, the investigators used appropriate records, selected by using EZ-FRISK, from a global database. The fundamental frequency of H/V ratios calculated using SHAKE 91 agrees remarkably well with the measured H/V resonance peaks using the Nakamura method. Therefore, microtremor method could accurately predict the fundamental resonance frequency.

The highest amplification values occupy the middle coast area, which is characterized by its relatively thick alluvium and beach deposits, while most of the region of interest has amplification values less than 2.0 for all the spectral periods considered. The low amplification values of ground motion were found to be at the areas occupied by the harzburgite and tertiary limestone rocks with almost negligible amplification. No ground motion amplification at spectral periods of 1.0 and 2.0 s is observed on the corresponding maps.

Ground surface seismic hazard maps are provided, with return period of 475 years, showing horizontal peak ground acceleration (PGA), and 0.1, 0.2, 0.3, 1.0, and 2.0 s spectral accelerations at the ground surface. The maps show that the ground surface seismic hazard level is moderate with expected PGA in the range of 0.059–0.145 g for 475 years return period. The maximum surface ground motion values are associated with the 5 % damped horizontal spectral acceleration with a period of 0.1 s (equivalent to natural frequency of one story houses).

The production of seismic hazard maps at the surface of the urban areas can be used to develop a variety of hazard mitigation strategies such as seismic risk assessment,

emergency response, preparedness, and land-use planning. These maps can help in designing buried lifelines such as tunnels, water and sewage lines, gas and oil lines, and power and communication lines. However, site-specific investigations to estimate design earthquake characteristics still need to be performed for the design of special and important buildings, and for rehabilitation and retrofit projects.

Acknowledgments The authors express their sincere appreciation to Oman Ministerial Cabinet for funding this project under project # 22409017. Thanks go also to Sultan Qaboos University for the strong support and encouragement and to the Seismic hazard committee members for their interest and assistance to complete this project.

References

Aki K, Richards PG (1980) Quantitative seismology. Freeman and Co., New York

Al Atik L, Abrahamson NA (2010) An improved method for non-stationary spectral matching. Earthq Spectra 26:601–617

Ambraseys NN, Melville CP, Adams RD (1994) The seismicity of Egypt, Arabia and Red Sea. Cambridge University Press, Cambridge

Anbazhagan P, Sitharam T (2008) Site characterization and site response studies using shear wave velocity. J Seismol Earthq Eng 10:53–67

Bindi D, Parolai S, Spallarossa D, Cattaneo M (2000) Site effects by H/V ratio: comparison of two different procedures. J Earthq Eng 4:97–113

Boore D (2008) Notes on smoothing over intervals that are constant over logarithmically-spaced frequencies. http://daveboore.com/daves_notes/notes%20on%20smoothing%20over%20logarithmically%20spaced%20freqs.pdf

Borcherdt RD (1970) Effects of local geology on ground motion near San Francisco Bay. Bull Seism Soc Am 60:29–61

BRGM/MPM (1986) Geological maps 1:100,000 scale, sheets Seeb and Muscat

Bullen KE (1963) An Introduction to the theory of seismology, 3rd edn. Cambridge University press, Cambridge

Cramer CH, Gomberg JS, Schweig ES, Waldron BA, Tucker K (2004) The Memphis, Shelby County, Tennessee, seismic hazard maps. U.S. Geological Survey Open-File Report 04-1294

Cramer CH, Gomberg JS, Schweig ES, Waldron BA, Tucker K (2006) First USGS urban seismic hazard maps predict the effects of soils. Seismol Res Lett 77:23–29

Dunand F, Bard PY, Chatelin JL, Guéguen Ph, Vassail T, Farsi MN (2002) Damping and frequency from random method applied to in situ measurements of ambient vibrations: evidence for effective soil structure interaction. 12th European conference on earthquake engineering, London. Paper# 869

El-Hussain I, Deif A, Al-Jabri K, Toksoz N, El-Hady S, Al-Hashmi S, Al-Toubi K, Al-Shijby Y, Al-Saify M, Kuleli S (2012a) Probabilistic seismic hazard maps for the Sultanate of Oman. Nat Hazard 64:173–210. doi:10.1007/s11069-012-0232-3

El-Hussain I, Deif A, Al-Jabri K, Al-Hashmi S, Al-Toubi K, Al-Shijby Y, Al-Saify M, Al-Habsi Z (2012b) Mitigation of seismic risk by microzonation Muscat Area, Sultanate of Oman, (Phase II). Project #22409017, submitted to Sultan Qaboos University, Oman

Idriss IM, Sun JI (1992) User's manual for SHAKE91, COMPUTER program for conducting equivalent linear seismic response analyses of horizontally layered soil deposits. University of California, Davis

Kanli A, Tildy P, Pronay Z, Pinar A, Hermann L (2006) V_{S30} mapping and soil classification for seismic site effect evaluation in Dinar region, SW Turkey. Geophys J Int 165:223–235

Konno K, Ohmachi T (1998) Ground motion characteristics estimated from spectral ratio between horizontal and vertical components of microtremor. Bull Seismol Soc Am 88:228–241

Kramer SL (1995) Geotechnical earthquake engineering. Prentice Hall, Inc., Upper Saddle River

Kramer SL (1996) Geotechnical earthquake engineering. Published by Pearson Education Ptd. Ltd, Reprinted 2003, Delhi, India

Lachet C, Bard PY (1994) Numerical and theoretical investigations on the possibilities and limitations of the Nakamura's technique. J Phys Earth 42:377–397

Lachet C, Bard PY (1995) Theoretical investigation of the Nakamura's technique. In: Proceedings of the 3rd international conference on recent advances in geotechnical earthquake engineering and soil dynamics, vol 2, pp 617–675

Lermo J, Chavez-Garcia FJ (1994) Are microtremors useful in site response evaluations? Bull Seismol Soc Am 84:1350–1364

Mahajan SS, Ranjan R, Sporry R, Champatiray PK, Westen CJV (2007) Seismic microzonation of Dehradun City using geophysical and geotechnical characteristics in the upper 30 m of soil column. J Seismol 11:355–370

Malagnini L, Tricarico P, Rovelli A, Hermann RB, Opics S, Biella G, de Franco R (1996) Explosion, earthquake and ambient noise recording in a Pliocene sediments-filled valley: inferences on seismic response properties by reference- and non-reference site techniques. Bull Seismol Soc Am 86:670–682

Miller RD, Xia J, Park CB, Ivanov J (1999) Multichannel analysis of surface waves to map bedrock. Lead Edge 18:1392–1396

Mohamed AME, Deif A, El-Hadidy S, Moustafa Sayed SR, El Werr A (2008) Definition of soil characteristics and ground response at the northwestern part of the Gulf of Suez, Egypt. J Geophys Eng 5:420–437

Nakamura Y (1989) A method for dynamic characteristics estimation of subsurface using microtremor of the ground surface. QR of RTRI, 30, No. 1, 89, Feb

Nakamura Y (1996) Real-time information systems for hazards mitigation. In: Proceedings of the 11th world conference on earthquake engineering, Acapulco, Mexico

NEHRP (2001) NEHRP recommended provisions for seismic regulations for new buildings and other structures (FEMA 368 and 369). 2000 ed. Building Seismic Safety Council, National Institute of Building Sciences, Washington, DC

Nogoshi M, Igarashi T (1970) On the propagation characteristics of microtremors. J Seismol Soc Jpn 23:264–280 (in Japanese with English abstract)

Nogoshi M, Igarashi T (1971) On the amplitude characteristics of microtremor (part 2). J Seism Soc Jpn 24:26–40 (in Japanese with English abstract)

Ohori M, Nobata A, Wakamatsu K (2002) A comparison of ESAC and FK methods of estimating phase velocity using arbitrarily shaped microtremor analysis. Bull Seismol Soc Am 92:2323–2332

Park CB, Miller RD, Xia J (1999) Multi-channel analysis of surface waves. Geophysics 64:800–808

Parolai S, Bindi D, Baumbach M, Grosser H, Milkereit C, Karakisa S, Zunbul S (2004) Comparison of different site response estimation techniques using aftershocks of the 1999 Izmit earthquake. Bull Seismol Soc Am 94:1096–1108

Picozzi M, Parolai S, Albarello D (2005) Statistical analysis of noise horizontal to vertical spectral ratios (HVSR). Bull Seismol Soc Am 95. doi:10.1785/0120040152

Safak E (1997) Models and methods to characterize site amplification from a pair of records. Earthq Spectra 13:97–129

Schnabel PB, Lysmer J, Seed HB (1972) SHAKE: a computer program for earthquake response analysis of horizontally layered sites, report no. UCB/EERC-72/12. Earthquake Engineering Research Center, University of California, Berkeley

Seed HB, Idriss IM (1970) Soil moduli and damping factors for dynamic response analyses. Earthquake Engineering Research Center, University of California, Berkeley, California, Rep. No. EERC-70/10

Seed HB, Wong RT, Idriss IM, Tokimatsu K (1986) Moduli and damping factors for dynamic analyses of cohesionless soils. J Geotech Eng 112:1016–1032

SeisRefa (1991) Refraction analysis program, version 1.30, USA. Copyright, Oyo Corporation

SESAME (2004) Site effects assessment using ambient excitations European research project. http://sesamefp5.obs.ujf-grenoble.fr

Seshunarayana T, Sundararajan N (2004) Multichannel analysis of surface waves (MASW) for mapping shallow subsurface layers—a case study, Jabalpur, India. 5th International Conference on Petroleum Geophysics, Hyderabad, India, pp 642–646

Seshunarayana T, Prabhakara Prasad P, Prasada Rao SVV, Kousalya M (2003) Seismic survey for determination of Vp and Vs of shallow subsoil & bedrock depth in Jabalpur area. Tech report No. NGRI-2003-Exp-384

Stokoe II KH, Wright GW, James AB, Jose MR (1994) Characterization of geotechnical sites by SASW method. In: Woods RD (ed) Geophysical characterization of sites: ISSMFE Technical Committee #10, Oxford Publishers, New Delhi

Street R, Woolery E, Wang Z, Harik IE (1997) Soil classifications for estimating site-dependent response spectra and seismic coefficients for building code provisions in western Kentucky. Eng Geol 46:331–347

Street R, Wooley EW, Wang Z, Harris JB (2001) NEHRP soil classification for estimating site dependant seismic coefficients in the Upper Mississippi Embayment. Eng Geol 62:123–135

Sundararajan N, Seshunarayana T (2011) Liquefaction hazard assessment of earthquake prone area: a case study based on shear wave velocity by multichannel analysis of surface waves (MASW). Geotech Geol Eng 29:267–275

Surve G, Mohan G (2010) Site response studies in Mumbai using (H/V) Nakamura technique. Nat Hazards 54:783–795

Theodulidis N, Bard PY (1995) Horizontal to vertical spectral ratio and geological conditions, an analysis of strong motion data from Greece and Taiwan (SMART-1). Soil Dyn Earthq Eng 14:177–197

Tian G, Steeples DW, Xia J, Miller RD (2003) Multichannel analysis of surface wave method with the auto juggie. Soil Dyn Earthq Eng 23:243–247

Tokimatsu K, Tamura S, Kojima H (1992) Effects of multiple modes on Rayleigh wave dispersion characteristics. J Geotech Eng 118:1529–1543

Xia J, Miller RD, Park CB (1999) Estimation of near-surface shear-wave velocity by inversion of Rayleigh wave. Geophysics 64:691–700

Xia J, Miller RD, Park CB, Ivanov J (2000) Construction of 2-D vertical shear wave velocity field by the multichannel analysis of surface wave technique. In: Proceedings of the symposium on the application of geophysics to engineering and environmental problems, Arlington, 20–24 Feb 2000

Xia J, Miller RD, Park CB, Hunter JA, Harris JB, Ivanov J (2002) Comparing shear-wave velocity profiles inverted from multichannel surface wave with borehole measurements. Soil Dyn Earthq Eng 22: 181–190

Zaslavsky Y, Shapira A, Gorstein M, Kalmanovich M, Giller V, Ion Livshits I, Alexander Shvartsburg A, Ataev G, Aksienko T, Dagmara Giller D, Ilana Dan I, Perelman N (2003) Local site effect of Hashefela and Hasharon regions based on ambient vibration measurements, Progress report, July, 2003, GII Report No. 569/313/03